Effects of redox variability and early diagenesis on marine sedimentary Hg records

J. Frieling [a],[*], T.A. Mather [a], C. März [b],[1], H.C. Jenkyns [a], R. Hennekam [d], G.-J. Reichart [c],[d], C.P. Slomp [c],[e], N.A.G.M. van Helmond [c],[e]

[a] Department of Earth Sciences, University of Oxford, Oxford, United Kingdom
[b] School of Earth and Environment, University of Leeds, Leeds, United Kingdom
[c] Department of Earth Sciences, Utrecht University, Utrecht, the Netherlands
[d] Royal Netherlands Institute for Sea Research (NIOZ), 't Horntje, Texel, the Netherlands
[e] Radboud Institute for Biological and Environmental Sciences, Radboud University, Nijmegen, the Netherlands

ARTICLE INFO

ABSTRACT

Volcanism is a dominant natural source of mercury (Hg) to the atmosphere, biosphere, ocean and sediments. In recent years, sedimentary Hg contents have emerged as a tool to reconstruct volcanic activity, and particularly activity of (subaerially emplaced) large igneous provinces in geological deep time. More specifically, Hg has shown potential as a useful proxy to illuminate the previously elusive impact of such large-scale volcanism on marine and terrestrial paleo-environments. While Hg is now widely applied as volcanism tracer, non-volcanic factors controlling sedimentary Hg content are generally not well constrained. Part of this uncertainty stems from our inability to directly observe a natural unperturbed "steady-state" environment as a baseline, as the modern Hg cycle is heavily influenced by anthropogenic activity. Here we focus on the effects of ambient redox conditions in the water column and shallow sediments (early diagenesis), quantify their influence on the geological Hg record and thereby contribute to constraining their potential impact on the use of Hg as a proxy for deep-time volcanic activity. Constraining these factors is of critical importance for the application of Hg as such a proxy. Many periods in the geological past for which records have been generated, such as the Mesozoic Oceanic Anoxic Events, are marked by a variety of high-amplitude environmental perturbations, including widespread deoxygenation and deposition of organic-rich sediments. We estimate the impact of redox changes and early diagenesis on the geological Hg record using a suite of (sub)recent–Pleistocene and Upper Cretaceous sediments representing oxic to euxinic marine conditions. Our sample set includes a transect through an oxygen minimum zone and cores that record transient shifts in oxygenation state, as well as post-depositional effects – all unrelated to volcanism, to the best of our knowledge. We find substantial alterations to the Hg record and the total organic carbon and total sulfur content, which are typically assumed to be the most common carrier phases of Hg in marine sediments. Moreover, these biases can lead to signal alteration on a par with those interpreted to result from volcanic activity. Geochemical modifications are ubiquitous and their potential magnitude implies that the factors leading to biases in the geological record warrant careful consideration before interpretation. Factors of particular concern to proxy application are (1) the disproportionate loss of organic carbon and sulfur relative to Hg during oxidation that strongly modulates normalized Hg records, (2) the evasion of Hg in anoxic and mildly euxinic sediments and (3) sharp focusing of Hg during post-depositional oxidation of organic matter. We suggest that paired analyses of additional redox-sensitive trace elements such as molybdenum, and organic-matter characteristics, particularly the type of organic matter, could provide first-order constraints on the role that redox and diagenetic changes played in shaping the Hg record as part of checking the attribution of enrichments to volcanic activity.

1. Introduction

In recent years, sedimentary mercury (Hg) has rapidly gained widespread attention due to its proposed use as a proxy for volcanic activity, particularly the volcanism associated with (subaerial) emplacement of large igneous provinces (LIPs) in the geological deep past ($\gg 10^6$ years) (e.g. Sanei et al., 2012; Grasby et al., 2013; Percival et al., 2017; Kender et al., 2021). This approach is based on the predominance of volcanically derived Hg prior to the emergence of anthropogenic fluxes (Pyle and Mather, 2003; Fitzgerald et al., 2007; Pirrone et al., 2010). Particular attention has been given to periods in geological time during which subaerial LIPs are thought to have been highly active, based on other sedimentary proxies (such as Os isotopes and (trace) metal enrichments; e.g., (Cohen et al., 2004; Snow et al., 2005; Du Vivier et al., 2014)) as well as direct dating of volcanogenic deposits (e.g., Sprain et al., 2019). These periods of (subaerial) LIP activity have also been studied for their high-amplitude environmental perturbations, including global warming, increased weathering, loss of biodiversity, changes in terrestrial vegetation, soil erosion, extensive water-column anoxia–euxinia and ocean acidification.

To make accurate inferences about volcanic LIP activity from Hg enrichments in stratigraphic records, the influence of other sedimentary changes on Hg and its carrier compounds needs to be resolved in appropriate detail. For example, it is well established that particulate and dissolved organic matter (OM) concentration is an important factor in governing the Hg levels in seawater (Wallace, 1982) and sediments (Fitzgerald et al., 2007; Gehrke et al., 2009). This relationship is due to the very high affinity of Hg^{2+} for OM and particularly organic sulfur functional groups (thiols) (see e.g. review of Ravichandran, 2004 and references therein), which commonly leads to strong correlations between total organic carbon (TOC) and Hg (Outridge et al., 2007; Gehrke et al., 2009). While there are some indications that, under extremely high productivity regimes, dilution of Hg by organic matter might play a role (Machado et al., 2016), such a mechanism appears to be uncommon in modern aquatic and sedimentary environments where Hg concentrations and Hg sequestration are positively correlated to (algal) OM abundance (profiles), although this relation is not necessarily linear (Wallace, 1982; Sanei and Goodarzi, 2006; Fitzgerald et al., 2007; Outridge et al., 2007; Bowman et al., 2016; Biester et al., 2018; Schütze et al., 2021; Cossa et al., 2022).

To eliminate variation induced by changes in OM content, normalizing Hg contents against TOC in sedimentary records has become common practice in the deep-time literature (e.g. Percival et al., 2015; Percival et al., 2017; Grasby et al., 2019; Jones et al., 2019; Shen et al., 2019b; Kender et al., 2021; Tremblin et al., 2022; Zhao et al., 2022). The basis for this approach lies in the evidenced assumption that Hg in the sedimentary record tends to be primarily bound to OM (including thiols) and only secondarily to other potential scavenging compounds (e.g., sulfides that form compounds such as mercury sulfide (HgS) or Hg inclusion in pyrite, or adsorption to clays), especially in the presence of abundant OM (e.g., Fitzgerald et al., 2007 and references therein). In the absence of large Hg-cycle perturbations, the positive correlation between Hg and TOC, both at single sample localities (e.g., Percival et al., 2015; Shen et al., 2020) and at broader scales (e.g., Grasby et al., 2019) in the geological record, provides support for this generalization. However, the relationship between Hg and TOC is in many instances not straightforward and since normalized Hg is not stable across all environments, the assumption that Hg/TOC (or otherwise normalized Hg) remains stable (in the absence of large-scale volcanic emissions) does not hold true for many deep-time records analyzed to date. Moreover, it has been established that, for example, other sedimentary Hg carrier phases such as sulfides (HgS) and (diagenetic) pyrite can be an important Hg-host in ancient sediments, especially when depositional conditions were strongly euxinic (Shen et al., 2019a, 2020; Wang et al., 2020). Critically, the association with diagenetic pyrite is a clear indication that Hg-speciation can change during diagenesis, which may complicate

assessment of the original Hg signal. Through association with TOC, clays and S, Hg might appear to behave in a similar way to bio-essential, redox-sensitive and/or sulfide-forming trace metals (such as, for example, Mo, V, Ni, Cd, Zn), that may change phase associations following their deposition at the seafloor (e.g., Tribovillard et al., 2006; Brumsack, 2006). Such processes complicate the direct use of water-column or modern-sediment Hg speciation data to make inferences of Hg cycling during early diagenesis and hamper understanding of the Hg signal captured in ancient sediment samples.

To date, variability in pre-industrial marine sediments, and particularly in deep-time records, related to the processes controlling coupled TOC, S and Hg burial, remains poorly understood. These processes can be roughly divided into two categories. In the first category are processes that influence Hg and/or TOC before they enter the sedimentary record, such as the riverine flux of Hg and terrestrial OM, ocean–atmosphere exchange, and water-column processes (abundance of marine OM, remineralization, scavenging efficiency). The second category includes processes that take place during or shortly after the sedimentary record is formed, particularly early diagenetic and soft-sediment processes: redox behavior, remineralization and remobilization. The cycling of Hg, the position of the redox front and its migration ultimately determine the signal preserved in the sedimentary record (Fig. 1).

The short-term processes that lead to the original Hg deposition in the marine realm, as well as early diagenesis, potentially influence any geological record of Hg and OM. Therefore, these processes warrant careful consideration in terms of what their effects might be and how they might be recognized. Because Hg, TOC and other Hg-binding ligands are unlikely to be uniformly influenced by early diagenesis, and particularly by oxidation, TOC- or total S (TS)-normalized records will be especially sensitive to these poorly constrained confounding factors. We here focus on the short-term post-depositional diagenetic alteration of Hg and its carrier phases (TOC and TS) and how such alteration might have influenced the sedimentary record.

Before applying the knowledge of Hg redox behavior in modern systems to the geological record, it is critical to recognize that this is based on recent and often polluted (soft) sediments (e.g., Fitzgerald et al., 2007; Gagnon et al., 1997). These sediments not only have temporally and spatially highly variable and uncertain Hg influxes (e.g., Covelli et al., 2001; Leipe et al., 2013; Mason et al., 1994), but, even if not heavily polluted, are also subject to ongoing oxidation and redox-front migration. As these modern environments are continuously being geochemically modified, also on time-scales beyond those that can be observed in controlled environments (10 s to >1000 s of years), the findings obtained from them cannot be directly applied to signals that are recorded in ancient sedimentary Hg records. Syn-sedimentary oxidation leads to progressive loss of sedimentary OM and S and, after oxygen-depletion, increased sedimentary reduced S from sulfide minerals (e.g. Berner, 1984). The sedimentary organic matter and S are themselves also interdependently altered during early diagenesis (Sinninghe Damsté and De Leeuw, 1990; Zaback and Pratt, 1992; Van Kaam-Peters et al., 1998; Werne et al., 2003; Raven et al., 2023). This complication implies that an accurate assessment of the most likely original binding spots for Hg, thiol groups, presents a major challenge for investigation ancient sediment samples. Moreover, as TOC and S are considered the most common Hg carriers in the geological record, the diagenetic and redox processes acting on the host phases themselves add a second layer of complexity to TOC- and TS-normalized Hg records. Constraining the behavior of Hg and its relationship to the most common carrier phases (TOC, S) under variable redox conditions and understanding how these signals are recorded in sediments is fundamental for the use of (normalized) sedimentary Hg as a direct proxy for Hg-cycle perturbations and volcanic activity.

Understanding the role of chemical changes associated with early diagenesis and (an)oxic degradation is particularly important because many of the key intervals in geological deep time for which enhanced
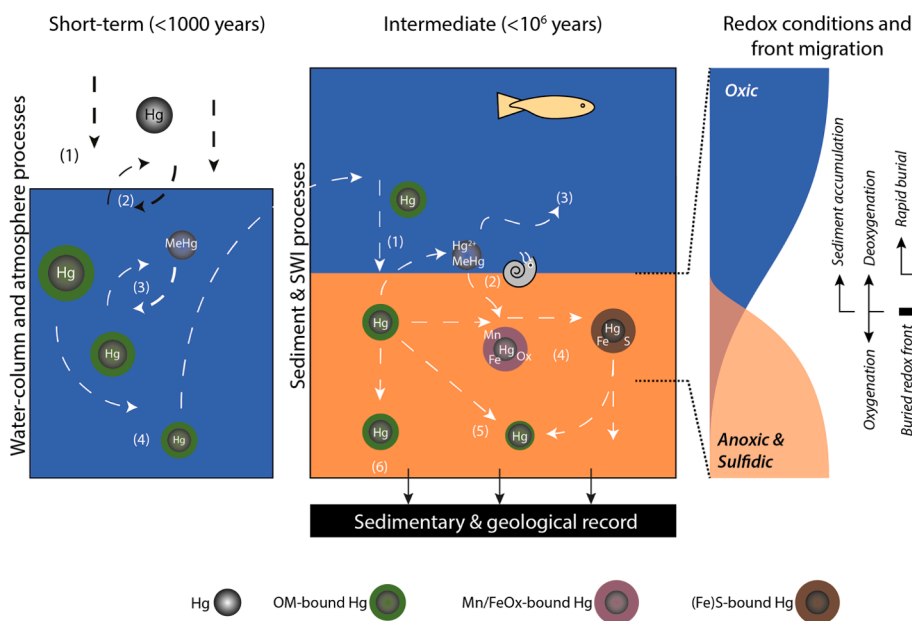
Fig. 1. Simplified diagram illustrating a selection of pathways that influence aquatic (marine) sedimentary mercury (Hg) and/or organic-matter cycling (green circles). Blue and brown/orange colors in middle panel indicate water and sediment, respectively.

Left-hand panel: atmospheric deposition and aquatic processes – (1) influx from rivers and atmosphere, (2) gaseous Hg exchange in the surface layer (Mason and Sheu, 2002; Strode et al., 2007; Mason et al., 2012), (3) uptake and remineralization of organic matter in the upper water column, and methylation-demethylation processes (MeHg) formation (Heimbürger et al., 2010), (4) progressive OM and Hg cycling and remineralization in the lower water column. Note that ageing deep water accumulates both C and Hg (Takahashi et al., 2002; Bowman et al., 2015, 2016).

Middle panel – processes potentially influenced by ambient oxygenation: (1) deposition of OM-bound Hg from the water column (Wallace, 1982) (2) bioturbation, diffusion and biologically driven cycling of OM and Hg near the sediment–water interface, (3) potentially resulting in Hg evasion (with MeHg or Mn/Fe (oxyhydr)oxides as intermediate phases) (Gagnon et al., 1997; Mikac et al., 1999; Hammerschmidt and Fitzgerald, 2004), (4) (temporary) binding to Mn/Fe (oxyhydr)oxides and sulfide minerals (Gagnon et al., 1997; Shen et al., 2020), (5) recalcitrant OM and Hg remaining after oxidation, (6) unaltered recording of Hg scavenged from the water column. **Right-hand panel - simplified reduction–oxidation (redox) front – controlling the position and intensity of processes depicted in the middle panel**. The redox front, here illustrated from the sediment–water interface down, migrates upwards with sediment accumulation and deoxygenation, downwards with (re) ventilation and may be buried and fixed, for example when a mass-transport deposit such as a turbidite rapidly covers the sediment–water interface (SWI). The position of the redox front influences many (trace-) element records and, combined with processes shown in the middle panel, such as Hg binding to Mn/Fe (oxyhydr) oxides, sulfides and methylation, conceivably also shapes the sedimentary Hg record.

volcanic activity is proposed were also marked by high-amplitude variations in primary productivity, (local) oxygenation and TOC contents in accumulating sediment (Schlanger and Jenkyns, 1976; Jenkyns, 2010; Ernst and Youbi, 2017). Some soft-sediment studies show that Hg could have been enriched at, or actively moved away from, (extinct) redox fronts, and microbial Hg methylation or Hg reduction could have resulted in active evasion from sediments and the water column (Mercone et al., 1999; Mikac et al., 1999; Fitzgerald et al., 2007, Fig. 1). We here consider resolving the paired geochemical behavior of Hg itself, and of its potential carrier phases, during early diagenesis. This knowledge is fundamental for the reliable use of Hg and normalized Hg as proxies for enhanced volcanism in geological deep time. Moreover, global, regional and local biogeochemical models that include or focus on the long-term (sedimentary) Hg cycle (e.g., Amos et al., 2013; Amos et al., 2015; Fendley et al., 2019; Dal Corso et al., 2020) benefit greatly from further data-driven constraints as to how Hg is sequestered on geological timescales. Ultimately, well-constrained behavior might facilitate inverse modelling of Hg fluxes and hence volcanic (Hg) emissions.

We designed our study to elucidate various influences of changing redox conditions on Hg, TOC and TS (and hence the most widely reported host phases of Hg records in the natural environment). To bridge the gap between soft-sediment processes and signals recorded in geological deep time, we generated new Hg and TOC data for a total of 10 depositional settings, 6 (sub)recent-Pleistocene and 4 Late Cretaceous ones (Fig. 2), representing a wide range of (paleo-)redox conditions and depositional environments (Fig. 2, Table 1). We relate these measurements to published major- and trace-element chemistry and associated inferred redox conditions. The redox conditions were generally reconstructed using Mo concentrations (Tribovillard et al., 2006; Lyons et al., 2009) and, in case of the recent sediments obtained from the Arabian Sea, assessed using pore-water chemistry and oxygen saturation of overlying bottom waters. We seek to eliminate major

influences on the Hg flux other than locally produced marine OM, changes in local oxygenation and inherited effects. To do so, we focus on geological intervals without known substantial subaerial LIP activity or nearby submarine LIP activity that may influence Hg records (Percival et al., 2018), and localities without substantial or variable input of terrestrial higher plant material that may have influenced Hg records (Them et al., 2019; Dal Corso et al., 2020). The main objectives of this study are to (1) establish whether variable oxidation leads to alteration in Hg and normalized Hg, (2) subsequently quantify any observed biases resulting from variable oxidation, and (3) resolve the origins of these biases.

2. Materials & methods

Materials – site descriptions.

2.1. Site selection

We first study the influence of natural long-term (10 s to 1000 s of years; Lengger et al., 2014) oxidation in a multi-core depth transect through the Arabian Sea oxygen minimum zone (OMZ) where it intersects the sea floor (Kraal et al., 2012). The three short (0–25 cm depth) cores (Stations 1B, 6B and 10; see also Kraal et al. (2012)) represent anoxic, hypoxic and oxic conditions respectively, and with the exception of Station 1B, where OM breakdown results from anaerobic processes, the uppermost sediments are subject to continued aerobic degradation. The observed differences between these sites can be attributed to oxidation in the water column and sediment and make the Arabian Sea OMZ an ideal testing ground for oxidation-induced sedimentary signals, including those in Hg and its carrier phases (see e.g., Kraal et al., 2012; Koho et al., 2013; Lengger et al., 2014 and Supplementary material 1.1) (Table 1a). In contrast to other records, where we rely on redox-proxy data, bottom-water oxygen saturation data and
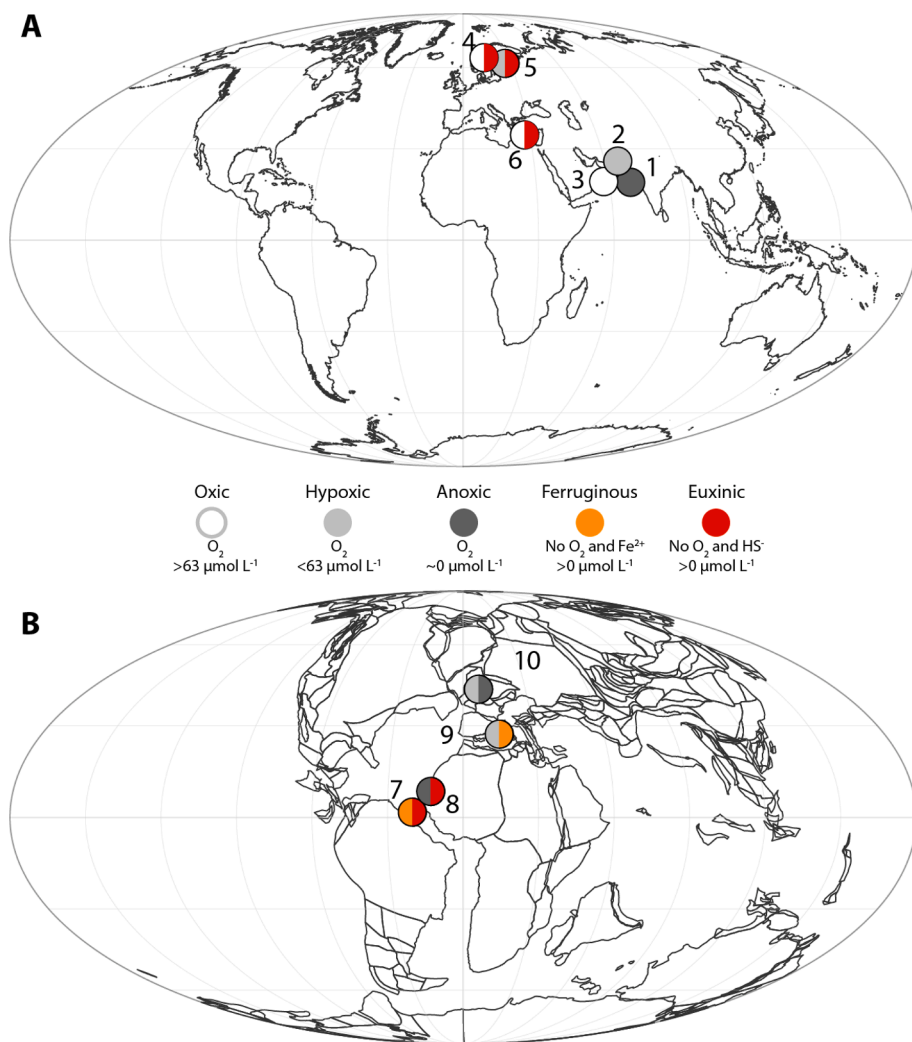
Fig. 2. **Maps of site locations. A.** Holocene–upper Pleistocene sites: (1, 2 and 3 Stations 1B, 6B and 10, Arabian Sea, (4 and 5) LL19, F80, Baltic Sea, (6) 64PE406-E1, Eastern Mediterranean Sea. **B.** Plate reconstruction for 90 Million years ago (Ma) with Cretaceous sites (7) ODP1261A Coniacian–Santonian Oceanic Anoxic Event (OAE 3; ~86 Ma) 3, (8) Cenomanian–Turonian (OAE 2; ~94 Ma) Tarfaya Basin core S57, Morocco, (9) Late Cenomanian, Furlo, Italy and (10) Cenomanian–Turonian (OAE 2) South Ferriby, United Kingdom. Colored symbols depict reconstructed bottom-water oxygenation from oxic (white), hypoxic (light grey – lowered oxygen conditions; $[O_2]_{aq} < 63$ µmol L^{-1}), anoxic (dark grey – oxygen-depleted conditions ~0 µmol L^{-1}), ferruginous (orange – no oxygen and Fe^{2+}) to euxinic (red – no oxygen and free HS^-). Differently colored semi-circles for a single site illustrate the approximate range of oxidation regimes within the analyzed sequence.

pore-water chemistry (Kraal et al., 2012; Vollebregt et al., 2023) are available to constrain the redox state of the Arabian Sea sediments.

Compared to the Arabian Sea multi-core data, the Baltic and Mediterranean Sea sediments cover transient redox variability, similar to reconstructions for many deep-time Hg records, and allow us to test how these changes in oxygenation shape the geological record of Hg and Hg carriers. To this end, we analyzed gravity-core material from the Baltic Sea, representing a time-series of the past 8 kyr (Supplementary material 1.2) (Jilbert and Slomp, 2013). These two cores, from the Fårö Deep (core F80) and Northern Gotland Basin (LL19), record oxic to euxinic bottom-water conditions and several transitions from oxic to euxinic and vice versa, within the same core (e.g., Jilbert and Slomp, 2013; van Helmond et al., 2018). The Baltic Sea cores thus provide insight as to how transitions in oxygenation might influence single sedimentary Hg records and to what extent such signals are preserved in the geological record (Table 1a). In addition, a multi- and piston-core composite site 64PE406-E1 in the Mediterranean Sea (Supplementary material 1.3), containing several Mediterranean sapropels, orbitally-paced products of run-off and productivity-driven anoxic phases (see e.g., Rohling et al., (2015) for a review of the Mediterranean sapropel records and their origin). Sapropel S1 and S5 are used here to further assess the influence of deoxygenation, post-depositional oxidation of organic-rich sediments and paleo-redox fronts (Mercone et al., 1999; Hennekam & van der Bolt et al., 2020; Sweere et al., 2021) (Table 1a). The post-depositional oxidation history of the sapropels was based on the decoupling of sedimentary Mo and Ba enrichment profiles. During organic-matter

oxidation, Mo is remobilized, while Ba is retained in the sediments providing a proxy for the oxidized part of the sapropels (Thomson et al., 1995; Reitz et al., 2006).

Lastly, we analyze four Upper Cretaceous successions to test whether the signals found in the oxic to sulfidic unconsolidated sediment are transferred to the rock record – on which sedimentary Hg studies targeting deep-time volcanic activity are based (Table 1b). For this purpose, we selected one Coniacian–Santonian black shale record from Ocean Drilling Program (ODP) Hole 1261A, Demarara Rise, equatorial Atlantic (März et al., 2008) (Supplementary material 1.4) recording cyclic alternations from ferruginous to sulfidic bottom-water conditions, and three upper Cenomanian to lowest Turonian successions (Furlo, Italy, South Ferriby, UK and Tarfaya core S57, Morocco) marked by high-amplitude variations in oxygenation (e.g., Poulton et al., 2015; Owens et al., 2017; Clarkson et al., 2018 and Supplementary material 1.5–1.7). The Cenomanian–Turonian successions might have been affected by contemporaneous LIP activity, but because the LIPs in question are thought to have been largely subaqueously emplaced and at substantial distance from the studied sites, the Hg-cycle perturbation is thought to be geographically confined even during periods of intense volcanism (Scaife et al., 2017; Percival et al., 2018).

2.2. Methods

2.2.1. Hg analyses
Prior to analyses, all samples were ground to fine powder, either by

Table 1a

Overview of studied Holocene and upper Pleistocene localities. For a more detailed description of each record refer to Section 1 of the supplementary text.

Site	Murray Ridge, Arabian Sea			Northern Gotland Basin, Baltic Sea	Fårö Deep, Baltic Sea	Eastern Mediterranean
Locality	Station 1B	Station 6B	Station 10	LL19	F80	64PE406-E1
No. on map	1	2	3	4	5	6
Period	Holocene	Holocene	Holocene	Holocene	Holocene	Holocene-late Pleistocene
Environmental setting	Open marine, upwelling zone (~900 m water depth)	Open marine, upwelling zone (~1500 m water depth)	Open marine, upwelling zone (~3000 m water depth)	Restricted, marginal sea (~170 m water depth)	Restricted, marginal sea (~190 m water depth)	Open marine (~1760 m water depth)
Oxygenation regime (s)	Anoxic	Hypoxic	Oxic	Oxic/hypoxic to euxinic	Oxic/hypoxic to euxinic	Oxic to euxinic
Accumulation rate	Moderate (1–10 cm/kyr)	Moderate (1–10 cm/kyr)	Moderate (1–10 cm/kyr)	Very high (>50 cm/kyr)	Very high (>50 cm/kyr)	Moderate (1–10 cm/kyr)
Data from literature	TOC, TS, trace elements (part), pore-water chemistry, Fe-speciation			TOC,TS, trace elements		TOC (part), trace elements
Key references	(Kraal et al., 2012; Lengger et al., 2014; Vollebregt et al., 2023)			(Jilbert and Slomp, 2013; van Helmond et al., 2018)		(Rush et al., 2019; Hennekam et al., 2020; Sweere et al., 2021)
Data generated	Hg	Hg	Hg	Hg	Hg	Hg, TOC (part)
Study aim	Resolve Hg & TOC accumulation in permanent strongly oxygen-depleted to oxic conditions, and relation to oxygenation in other sites with similar export flux (St. 1B, 6B and 10). Excludes temporal & spatial variability as a factor in shaping Hg records			Resolve Hg & TOC accumulation during transitions from oxic/dysoxic to euxinic conditions and vice versa, includes temporal variability. LL19 and F80 together provide control on potential spatial variability.		Isolate post-depositional oxidation including buried redox fronts.
Isolated factors	Oxygenation			Transient variability in oxygenation		Post-depositional oxidation
Potential processes reflected in sedimentary signals	Hg sequestration with organic matter and/or sulfur, Hg evasion	Hg sequestration with organic matter, subsequent slow break-down of organic matter and impact on Hg/TOC	Hg sequestration with organic matter, subsequent break-down of organic matter and impact on Hg/TOC	Hg sequestration with organic matter and sulfur, Hg focusing with sulfides, Hg evasion		Hg sequestration with organic matter and sulfur, Hg focusing with sulfides, Hg evasion, Hg focusing on redox fronts

Table 1b

Overview of studied Cretaceous localities. For a more detailed description of each record refer to Section 1 of the supplementary text.

Site	Demarara Rise, Equatorial Atlantic	Morocco	Italy	United Kingdom
Core/Locality	ODP1261A	Tarfaya S57	Furlo	South Ferriby
No. on map	7	8	9	10
Period	Coniacian-Santonian	OAE 2 interval	Cenomanian (pre-OAE 2)	OAE2 interval
Environmental setting	Open marine (semi-restricted)	Open marine, upwelling zone (?)	Open marine	Marginal sea
Oxygenation regime(s)	Ferruginous to euxinic	Ferruginous to euxinic	Hypoxic to euxinic	Oxic to hypoxic/anoxic
Sediment accumulation rate	Low-moderate (~1 cm/kyr)	Low-moderate (~1 cm/kyr)	Very low-low (<1 cm/kyr)	Very low (≪1 cm/kyr)
Data from literature (paired data only)	TOC, TS, trace elements			
Key references	(März et al., 2008)	(Tsikos et al., 2004; Poulton et al., 2015)	(Jenkyns et al., 2007; Owens et al., 2017)	(Jenkyns et al., 2007; Pogge Von Strandmann et al., 2013)
Data generated for this study	Hg, TOC (part)	Hg, TOC	Hg, TOC	Hg, TOC
Study aim	Test if geological deep time sedimentary successions record similar effects as seen in Holocene-Pleistocene records and if those effects can be traced to individual processes			

hand with an agate mortar and pestle or in a ceramic ball-mill. Mercury (Hg) analyses were conducted with a Lumex 915+ device, attached to a pyrolysis unit (PYRO-915) at the University of Oxford. For each sample, approximately 50–200 mg of homogenized powdered sediment was pyrolyzed at 700 °C and ~60% of samples were analyzed in duplicate to assess reproducibility. Calibration of the Lumex 915+ unit was performed using a paint-contaminated soil standard (NIST2587), which contains 290 ppb (ng/g) Hg. Reproducibility, established from long-term observations of this standard over the last 2 years ($n = 390$) was on average 6% when >3 ng Hg was analyzed. Given an effective maximum capacity of *ca.* 300 mg of the sample boats, this reproducibility estimate is valid for samples with >10 ppb Hg. A few samples with very low Hg contents (<5 ppb), closer to the detection limit, have analytical uncertainty >10%. With the exception of the Mediterranean core (64PE406-E1), all Hg was analyzed on sample powders that have also been analyzed for TOC, S and trace elements. For 64PE406-E1, we utilize a combination of calibrated Mo concentrations from X-ray fluorescence (XRF) scanning (Hennekam et al., 2020) and new and existing dedicated TOC measurements on the same powders that were analyzed for Hg.

2.2.2. Determination of organic and inorganic carbon

For black shales and samples expected to be relatively rich in organic carbon, total organic carbon (TOC), hydrocarbon yield of the organic matter and inorganic carbon were assessed with a Rock-Eval 6 device (Lafargue et al., 1998; Behar et al., 2001) at the University of Oxford. For every 10 samples, at least one in-house standard of homogenized sediment with pre-determined values was analyzed to assess reproducibility (2.72% TOC, standard deviation 1% of the measured value, $n = 20$). The reproducibility of other parameters of interest ($T_{max} = 0.5\%$ of measured value, Hydrogen Index (HI) = 2.2%, mineral carbon = 2.4%) was based on the same measurements of the in-house standard. The hydrogen index (HI) and oxygen index (OI) are used as in, e.g., Behar et al., (2001); briefly, the mass of released hydrocarbons ("S2") and CO_2 ("S3") during standard pyrolysis in mg is multiplied by 100 and divided by TOC to obtain HI and OI, respectively. Analyses of a decarbonated standard

(~48% carbonate) suggest that TOC, S2, S3 and consequently HI and OI were not significantly impacted by low-temperature decomposition of carbonates (Hazra et al., 2022). As all tested samples are dominated by marine organic matter (see Supplementary materials (S1.2–1.7)), we interpret HI and OI primarily as indicator of organic matter degradation. A subset of samples were previously analyzed for TOC using various established practices. TOC results determined after an acid-washing procedure (März et al., 2008) were here re-analyzed with Rock-Eval (ODP Hole 1261A) to confirm reproducibility. Average TOC is slightly higher (n = 39, 8.2 ± 1.4%) for acid-washed than for bulk RockEval analysis (7.5 ± 1.3%), confirming that there is minimal influence of methodology on the measured TOC content (Nieuwenhuize et al., 1994).

Organic-lean carbonates from the Furlo section were analyzed on a Strohlein Coulomat 702 at the University of Oxford. Total carbon of the bulk sediment was determined by analyzing 20–40 mg of untreated homogenized powdered material, while a second 20–40 mg aliquot was heated to 450 °C in a combustion furnace overnight to remove organic carbon. During analysis, combustion of the untreated and furnaced sample at ~1300 °C releases all carbon from the sample, which is then quantified via back-titration. The difference between the untreated sample and furnaced sample indicates the TOC content, whereas the heated aliquot represents the total inorganic carbon fraction (TIC). Long-term analytical reproducibility based on an in-house pure carbonate standard was determined to be ~0.1% C, while the detection limit is ~0.1% C. Total organic carbon measurements obtained from the RockEval 6 and Coulomat at the University of Oxford are routinely cross-checked with in-house standards.

A subset of samples (25) from the 64PE406-E1 multi- and piston core were analyzed for TOC at Royal Netherlands Institute for Sea Research (NIOZ). Samples were dried, homogenized, decarbonated with 2 M HCl and subsequently dried and homogenized again, followed by measurement on a Thermo-Interscience Flash EA1112 Series Elemental Analyzer. Based on replicate analyses of standard materials the accuracy is ~0.3% for TOC, with a detection limit of ~0.1%.
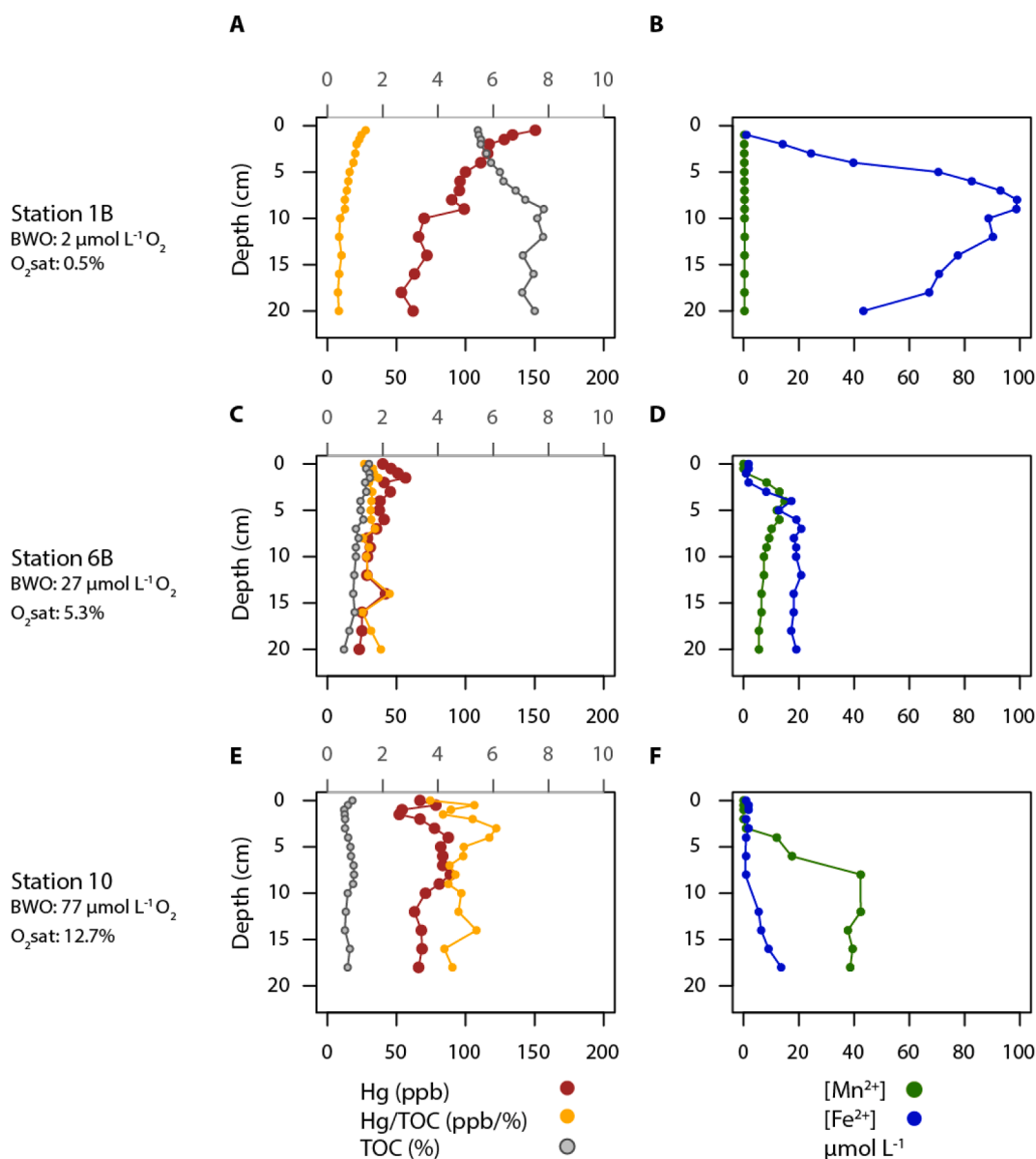

Fig. 3. Hg, TOC and sediment and pore-water chemistry for the Holocene (~0–4 ka) Arabian Sea stations. A, C, E. Hg, TOC and Hg/TOC for Station 1B, 6B and 10, respectively. Note that the TOC scale is on the top of each panel. B, D, F. Mn²⁺ and Fe²⁺ concentrations in pore waters. Bottom-water oxygen concentration (BWO) and saturation (O₂sat) for each station (Koho et al., 2013). TOC and pore-water data were published in Kraal et al. (2012).

2.2.3. Determination of Pb and Zn

For a small subset of samples ($n = 18$ from the Arabian Sea, sedimentary lead (Pb) and zinc (Zn) content were determined by analyzing the 1 M HCl total digestion extracts of Kraal et al. (2012) on an Inductively Coupled Plasma Mass Spectrometer (Thermo Fisher Scientific XSERIES 2 ICP-MS) at Utrecht University. The accuracy (recovery), based on QCs, was 99% for both Pb and Zn. Average analytical uncertainty based on sample replicates ($n = 6$) was 1.4% for Pb and 3.6% for Zn.

3. Results

3.1. Natural long-term oxidation – Arabian Sea

At the three Arabian Sea stations, Hg contents are highest at the top of Station 1B (the shallowest water station), with a maximum of 150 ppb, and lowest (23 ppb) for the lowermost sample of the Station 6B core (Fig. 3). Station 10 (greatest water depth) shows rather stable Hg contents (50–90 ppb). The elevated Hg contents at the top (<10 cm) of the anoxic station (1B) seem to suggest some influence of anthropogenic pollution. There are, however, several reasons why we consider anthropogenic contamination unlikely even at the top of the Station 1B core. For example, the elevated Hg does not appear in similar fashion at the other locations, and the average accumulation rates ($\sim$5–10 cm kyr^{-1}) would imply significant Hg perturbation prior to the industrial revolution (Koho et al., 2013). Furthermore, there is a complete absence of anomalous values in other commonly Hg-pollution-associated heavy metals such as Pb and Zn (Supplementary data). Lastly, there is no clear evidence for a trend break in Hg or Hg/TOC similar to the youngest part of the Baltic Sea cores (Fig. 3A, C); in the Arabian Sea Station 1B and 6B Hg content gradually decreases with depth. Hg overall correlates positively with TOC when all data from the three stations are combined ($R^2 \sim 0.3$, $p < 0.001$; Supplementary Fig. 1A), and the correlation coefficient increases when the two deeper water stations are considered individually (Station 6B, $R^2 \sim 0.7$, $p < 0.001$) and Station 10, $R^2 \sim 0.45$, $p = 0.004$). A negative correlation ($R^2 \sim 0.7$, $p < 0.001$) with TOC is found at the shallowest water Station 1B, which may be related to preferential (ongoing) Hg loss (paragraph 4.1.1), paired with a slight increase in TOC at the bottom of the core, that may be related to higher productivity at the time of deposition. The TOC profile here does not reflect organic-carbon loss, which is minimal compared to the particle flux (see also paragraph 4.1.1), which leads us to believe that the negative correlation with Hg is in part forced by small variations in the TOC flux.

Mercury and Hg/TOC for the shallowest water station (1B) show a strong decreasing trend with depth, as Hg reduces from 150 to 60 ppb whereas TOC increases from $\sim$5.5% to 7.5% (Fig. 3A). These opposing trends result in a strong negative correlation. Mercury at the intermediate station (6B) shows a similar, albeit much shallower, trend (Fig. 3C) but clear depth-dependent patterns in Hg/TOC are not recorded here or at Station 10 (Fig. 3C, E). Dissolved Mn (assumed to be Mn^{2+}) and Fe (assumed to be Fe^{2+}) constrain redox conditions for the Arabian Sea Stations. At Station 1B, the absence of dissolved Mn and presence of dissolved Fe shows that reduction of Fe-oxides is presumably the primary pathway for the (microbial) degradation of organic matter throughout the studied interval (Fig. 3B) (Kraal et al., 2012). Kraal et al. (2012) also determined that Mn-oxide reduction is more prevalent at Station 6B and becomes the dominant anaerobic pathway for (microbial) degradation of organic matter at Station 10 (Fig. 3D, F).

Across the site transect, average Hg/TOC increases markedly with oxygenation; we find Hg/TOC of 15 ± 6 ppb/% (mean, standard deviation, $n = 17$) at the shallowest (anoxic) site (Station 1B) (Fig. 3A), rising to 32 ± 5 ($n = 18$) at the intermediate (6B) (Fig. 3C) and 96 ± 12 ($n = 18$) at the deepest, most oxic site (10) (Fig. 3E). Arguably, the lowermost (i.e., greatest core depth) recovered sediments, where trends with depth are minimal in Hg and TOC, are most representative of the burial signal.

Focusing on the lowermost 10 cm of each core, we find a further decrease in Hg/TOC in the anoxic site to 8.7 ± 0.9 ($n = 6$), whereas Hg/TOC at the other sites remains virtually unchanged from top to bottom of the analyzed interval.

3.2. Influence of transient changes in oxygenation: Baltic Sea soft sediments

The Holocene sediment cores F80 and LL19 from the Baltic Sea (See Table 1, see Supplementary text 1.2 for details on age-depth models and previous studies using F80, LL19) show identical trends in TOC-normalized Hg and Hg content throughout. In the pre-industrial (<1750 calendar years common era (CE), based on the detailed age model of Jilbert and Slomp (2013), sedimentary Hg content did not exceed 40 ppb, whereas it reached a maximum well above 200 ppb around $\sim$1980 CE. Core F80 seems to record a subtle increase in Hg and Hg/TOC from about 1100–1200 CE, suggesting that, for example, small-scale early industrial activity or deforestation around the Baltic Sea may have influenced Hg influx at our sites, as is also supported by the Pb record in the study by van Helmond et al. (2020). The pre-industrial Holocene Hg and TOC contents in our cores are very similar to those obtained during earlier work in the Baltic Sea that focused mainly on the recent centuries and effects of modern anthropogenic Hg pollution (Leipe et al., 2013).

Before the main period of anthropogenic Hg emissions (<1750 CE), Hg loading in the oxic–anoxic sediments, based on correlation with TOC, appears to be almost completely controlled by their TOC contents (Supplementary Fig. 2A, C). In some anoxic–sulfidic intervals, TOC spikes above 10%, whereas the more oxic intervals generally have 1–2% TOC (Jilbert and Slomp, 2013). Hg/TOC averages $\sim$3.8–5.5 ppb/% in the anoxic to sulfidic intervals and averages 6.4 (F80) to 8.6 (LL19) in the more oxic intervals (Figs. 4, 6B, C). The non-sulfidic intervals at F80 show elevated Mo and lower Hg/TOC compared to the same intervals in LL19 (Fig. 4). This pattern may signal continued oxygen deficiency at F80 even during the most oxic phases, which is supported by sedimentary Re content data (van Helmond et al., 2018). Prior to the emergence of overwhelming Hg pollution (1750 CE), negative correlations between both Hg and Hg/TOC and redox-sensitive elements (Mo, U, Cd etc.) are ubiquitous. Such redox-sensitive elements are usually also enriched or proportional to the TOC values, whereas the rise in Hg is smaller than that in TOC (Fig. 4). This relationship implies that the correlation of other TOC-bound elements with Hg is generally positive and that the correlation of these elements with Hg/TOC is negative, as also indicated by the decreasing Hg/TOC with TOC. The negative correlation between sulfide-bound elements (Mo) and Hg/TOC weakens with increasing Mo, which suggests a non-linear connection between anoxic and especially sulfide-enriched (pore) waters and decrease in Hg/TOC (Fig. 4E, F).

3.3. Influence of post-depositional oxidation: Mediterranean Sea soft sediments

The sapropels S1 and S5 in sediments from the Eastern Mediterranean Sea show increased Hg contents compared to background sedimentation (Fig. 5). However, (slightly) subdued or stable Hg/TOC values appear in the anoxic intervals (high Mo, high Ba; for details on oxygenation during sapropel deposition see, e.g., Hennekam et al., 2020; Clarkson et al., 2021; Sweere et al., 2021), similar to the Arabian and Baltic Sea records. Background Hg contents in the oxygenated (low Mo, low Ba) sediments are $\sim$10 ppb, increasing to relatively stable values around $\sim$50 ppb (S1) and $\sim$100 ppb (S5) within the sapropel layers. The profiles also show second-order variability both below and above the sapropel layers. For example, the top of both S1 and S5 is marked by a clear spike in Hg contents (up to $\sim$100 ppb in S1 and $\sim$230 ppb in S5), approximately double the Hg contents observed in the lower part of the sapropels. These spikes are not paralleled by an accompanying increase in TOC, which remains stable around the average of the sapropel
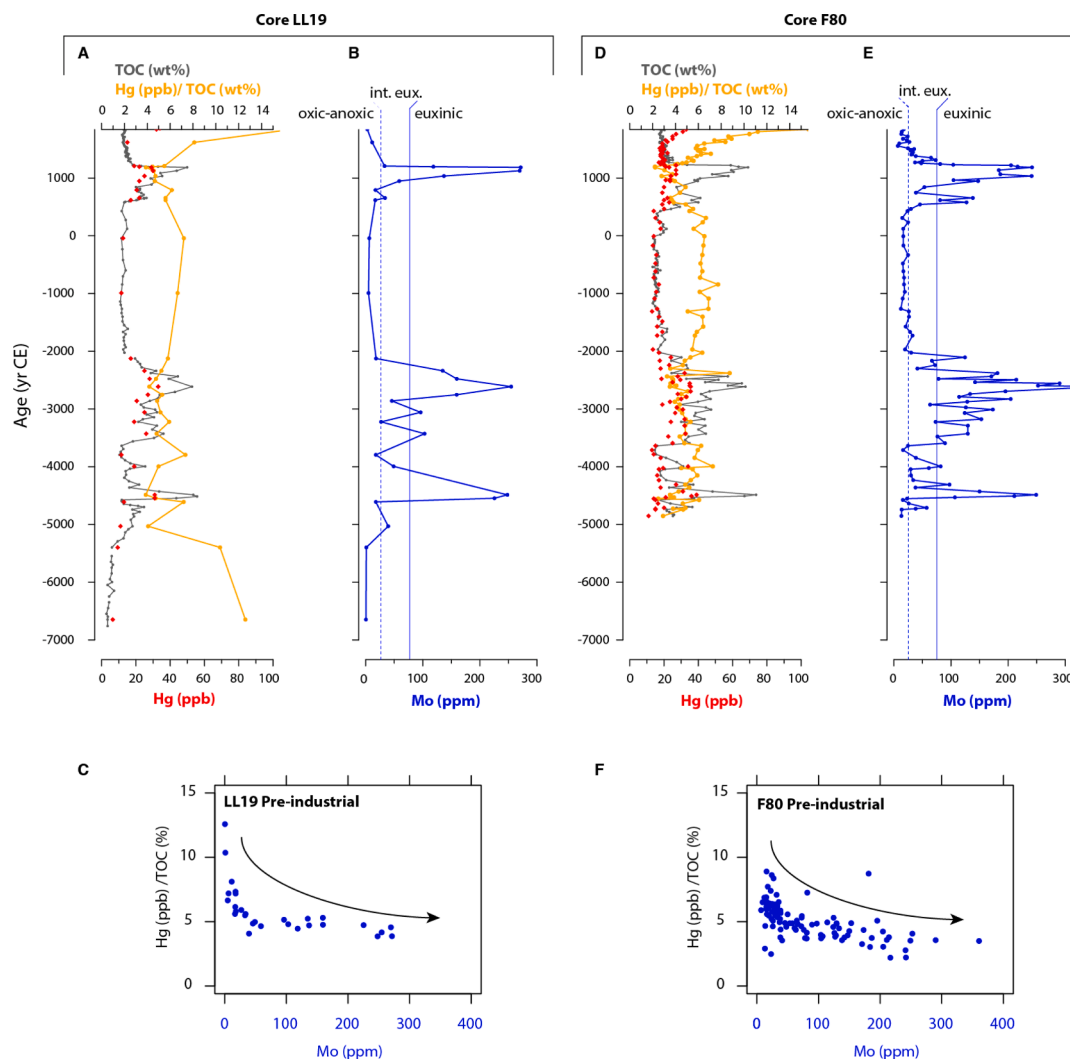
Fig. 4. Hg, TOC, and trace-element records for Baltic Sea cores LL19 and F80 for the Holocene (~0–8 ka). A. Hg, TOC and Hg/TOC for core LL19, North Gotland Basin. B. Molybdenum (Mo) contents for LL19 (data from van Helmond et al. 2018). C. Pre-industrial (<1750CE) Hg/TOC vs Mo for core LL19. D. Hg, TOC and Hg/TOC for core F80, Fårö Deep. E. Mo contents for F80 (data from van Helmond et al. 2018). F. Pre-industrial (<1750CE) Hg/TOC vs Mo for core F80. Abbreviation – int. eux. = intermittent euxinic conditions. Note that the top of the interval (>1500 CE) is marked by progressively increasing Hg and normalized Hg due to pollution.

interval (values around 1.5–2% in S1 and 5–6% in S5), above background values of ~0.5–1%. In general, the preserved Hg/TOC ratios are more variable (Figs. 5C, 6D) in background sediments than in sapropels. However, whether Hg/TOC values of the background deposits are higher than those of the sapropels, as suggested by the trends across the onset of sapropel S5, cannot be confidently determined with the available data.

Intriguingly, Hg/TOC for S1 is higher (~25 ppb/%) than for S5 (~17 ppb/%), which may be linked to more intense deoxygenation during S5 (Sweere et al., 2021) (see also Mo content in Fig. 5B and 5E). In the oxidized part of S1, where high Ba is considered to follow the original extent and intensity of the sapropel (e.g. van Santvoort et al., 2002) (ca. 28–23.5 cm depth, 8.3–6.5 ka), Hg spikes and Hg/TOC remains at a relatively elevated level. This pattern contrasts with TOC, of which a substantial part has been removed during post-depositional oxidation: the oxidized part of S1 records 0.8% TOC, whereas the unoxidized part records 2%. A similar effect appears to occur at the upper 3–4 cm of S5 (ca. 122 ka).

3.4. Influence of transient oxygen variability: The deep-time sedimentary record

3.4.1. Coniacian–Santonian, Ocean Drilling Program (ODP) Site 1261A

The Coniacian–Santonian sediments at Demarara Rise ODP Leg 207 Site 1261 Hole A (Shipboard Scientific Party, 2004) (Fig. 7) show generally high to very high TOC (4–12%) and moderate Hg content (20–140 ppb), compared to geological averages (~60 ppb for shales, ~30 ppb for limestones, Grasby et al., 2019). We find no obvious correlation between Hg and TOC or Hg and S (Supplementary Fig. 3), and see a pronounced cyclicity in Hg, Hg/TOC and Hg/TS. Hg/TOC ratios vary between ~5 ppb/% in some parts of the sulfidic intervals (as determined by März et al. 2008), and locally spike up to 15 ppb/% in the anoxic non-sulfidic intervals (shaded bands in Fig. 7) and directly above. Both the carbonate content and the carbonate-free TOC are lowest in the anoxic non-sulfidic sediments. Although Hg and TOC only weakly correlate, the HI and OI are negatively and positively correlated to Hg and that leads to a correlation of HI and OI with Hg/TOC (Fig. 7, 8D), suggesting organic-matter characteristics play an important role in shaping Hg and Hg/TOC. The negative correlation between Hg and Hg/TOC, marking Hg depletion relative to both (carbonate-free) Mo and TOC, are also observed here, similar to the Baltic Sea sites (Figs. 4E, 4F,
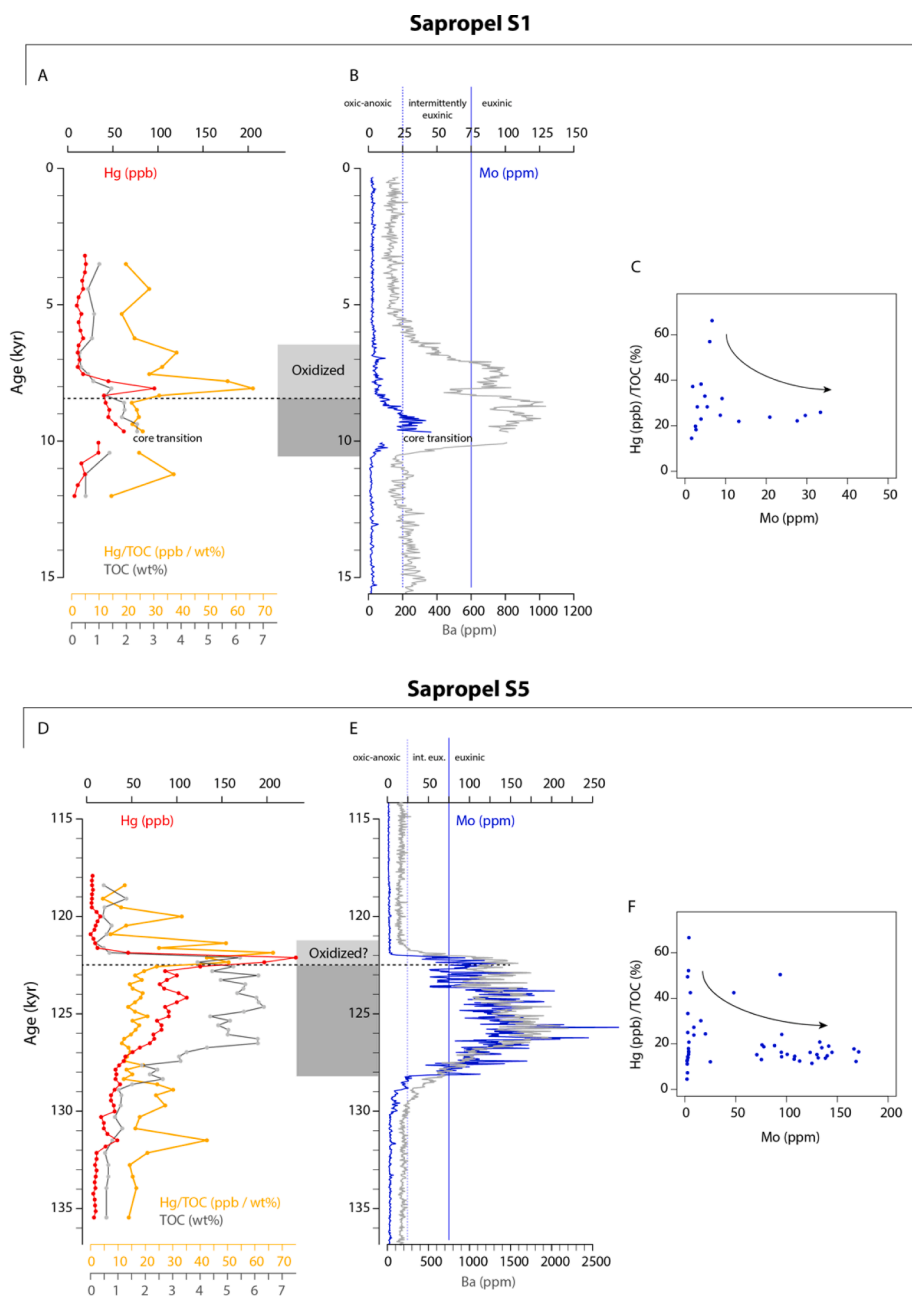
Fig. 5. Hg, TOC and trace-element records for 64PE406-E1 through intervals encompassing Sapropel S1 (deposited *ca.* 10.5–6.1 ka) and S5 (deposited *ca.* 128.3–121.5 ka). **A.** Hg, TOC and Hg/TOC for sapropel S1. **B.** Molybdenum (Mo) and barium (Ba) contents in ppm from calibrated high-resolution XRF scanning (data published in Hennekam & van der Bolt, et al. 2020). **C.** Hg/TOC vs Mo for the sapropel S1 interval. **D.** Hg, TOC and Hg/TOC for sapropel S5. **E.** Mo and Ba in ppm from calibrated high-resolution XRF scanning (data published in Hennekam & van der Bolt et al., 2020). **F.** Hg/TOC vs Mo for the sapropel S5 interval. Note that the dark shaded boxes in A and D show the extent of the unoxidized sapropel interval based on Mo content. The light shaded box shows the oxidized sapropel interval based on persistent elevated Ba content.

7E). The carbonate-corrected aluminum (Al) content is remarkably constant, suggesting stable Al accumulation rates throughout the analyzed interval. We find that Hg/Al follows the same pattern as Hg: a crucial observation that shows Hg burial was not constant and not driven primarily by Hg associated with an increased influx of siliciclastic material. As the higher Hg contents coincide with sediments containing evidence for ferruginous conditions (based on Fe-speciation data (März et al., 2008)), suggesting that Hg scavenging under such conditions was more efficient compared to euxinic conditions and/or that the sediments deposited under euxinic conditions lost (more) Hg.

3.4.2. Cenomanian, pre-OAE 2 level, Furlo, Italy

We here focus on organic-matter characteristics because paired trace-element records are not available for the selected samples, the bulk of the succession being represented by organic-lean white pelagic carbonates of the Scaglia Bianca (carbonate content 90–95%) and the remainder being represented by thin (centimeter-scale) black and green

shales and black cherts, with variable but generally much lower carbonate content (0–80%). Overall, these sediments also show large differences in TOC and Hg content, and notably Hg/TOC (Fig. S5). The latter could be partly a consequence of TOC and Hg often being difficult to measure reliably in the carbonates (see also Supplementary text S2). In the more organic-rich facies, where such analytical issues do not play a role, Hg/TOC ranges from 17 to >400, compared to 30 to 350 obtained by Percival et al. (2018). The overall correlation between Hg and TOC in the shales and cherts is strong ($R^2 \sim 0.7$, $p < 0.001$, Fig. S5D) while, after normalizing Hg to TOC, only a weak correlation with HI remains ($R^2 = 0.2$, $p = 0.02$), indicating that the type and/or preservational state of organic matter here has no dominant influence on Hg/TOC (Fig. 8A).

3.4.3. Cenomanian–Turonian (OAE 2), S57 core, Tarfaya, Morocco

The TOC content of the S57 core samples from Tarfaya, Morocco, is consistently high (average 7%) and never drops below ~1% in the studied core interval (50–60 m core depth) (e.g., Tsikos et al., 2004;
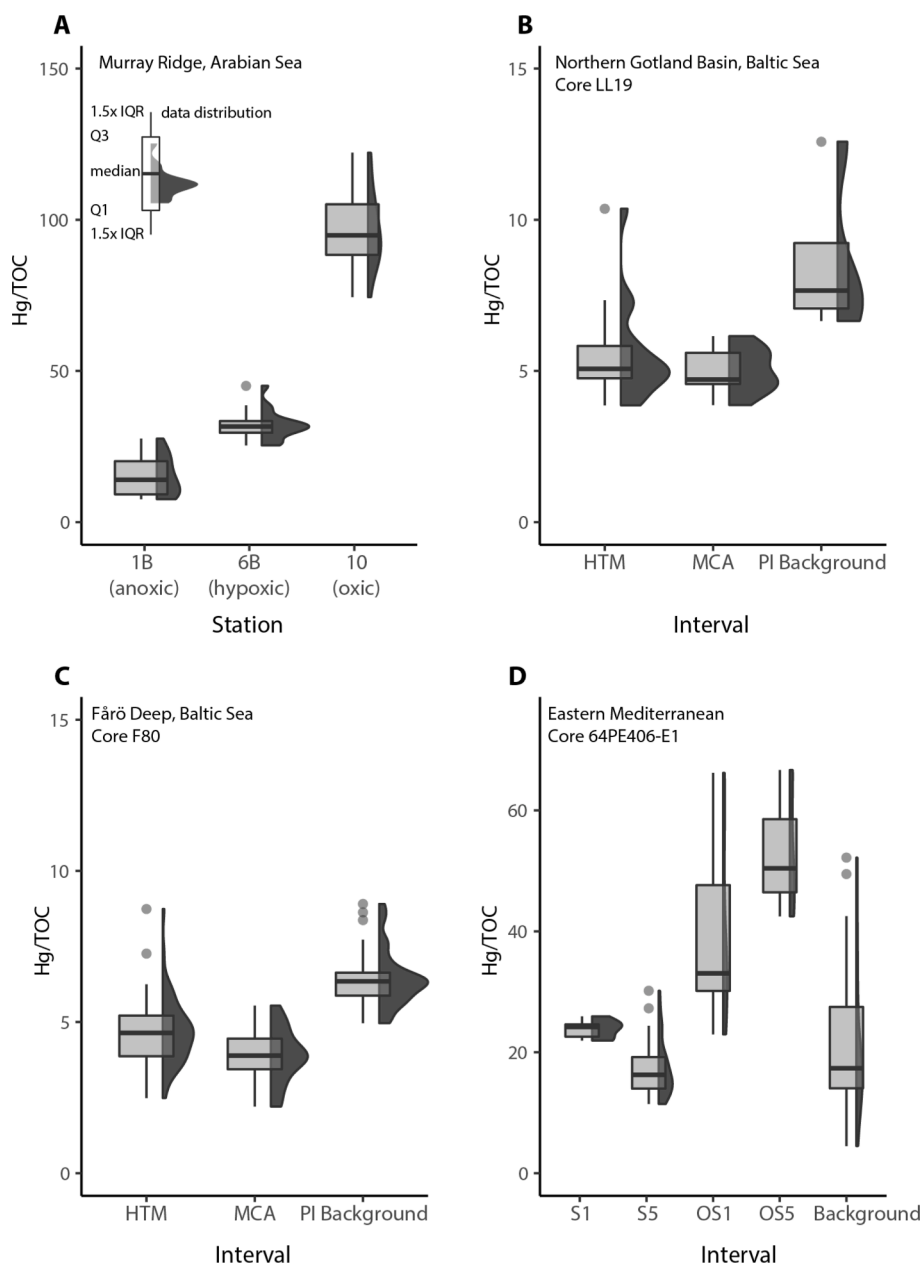
Fig. 6. Summary of observed Recent to upper Pleistocene Hg/TOC in the Baltic, Arabian and Mediterranean Sea cores. A. Hg/TOC for the Arabian Sea stations, going from anoxic (1B) to oxic (10). **B.** Hg/TOC for the Holocene Thermal Maximum (HTM; *ca.* 5000 – 2000 BCE) and Medieval Climate Anomaly (MCA, *ca.* 500 – 1200 CE) euxinic and pre-industrial (PI) oxic background intervals for core LL19. **C.** As panel B but for core F80. **D.** Hg/TOC for Site 64PE406-E1, Eastern Mediterranean, split by oxidation regimes: sapropels "S1", "S5", their oxidized tops, "OS1" and "OS5", and background.

Percival et al., 2018). The TOC and Hg data used here are from Percival et al. (2018) and oxygenation for the sample levels is estimated based on Fe speciation and lipid biomarkers (Poulton et al., 2015). We here record high HI values, above 500 and average ~660, indicative of immature marine organic matter. Hg and TOC are well correlated across the entire analyzed interval (Percival et al., 2018). Hg/TOC values are generally low, averaging ~23 (min 9.5, max 88) and correlate moderately well ($R^2 \sim 0.4$, $p < 0.001$) with the OI but not significantly with HI ($R^2 \sim 0.1$, $p = 0.11$), suggesting that either preservation or a (small) refractory organic-matter pool plays a role in shaping Hg/TOC relationships. Across the ferruginous–euxinic cyclic variations, only small changes in Hg/TOC are observed, and correlation between Hg/TOC and OI in this interval is somewhat weaker than across the entire interval previously analyzed for Hg and TOC (Percival et al., 2018).

3.4.4. Cenomanian–Turonian (OAE 2), South Ferriby Black Band, UK

Hg contents across the South Ferriby Black Band range from 40 ppb in the pelagic white chalk to 350 ppb in the black-shale interval that is

the hallmark of OAE 2. A weak and insignificant correlation ($R^2 = 0.16$, $p = 0.1$, Fig. S4B) with TOC is found but the negative correlation of Hg/TOC with HI ($R^2 = 0.55$, $p = 0.02$) and the positive correlation with OI ($R^2 = 0.88$, $p < 0.001$) are stronger (Fig. 8C). TOC in the pre-event carbonate-rich sediments is ~0.2%, reaching a maximum of 6–7% in the Black Band itself (Jenkyns et al., 2007). Hg/TOC ratios decrease from values above 200 ppb/wt % in the organic-lean carbonates below the Black Band to an average of ~45 ppb/wt % in the black shale. Minimum Hg/TOC coincides with the highest TOC contents and HI/OI indicates that the best-preserved (marine) organic matter shows lowest Hg/TOC (Fig. 8C).
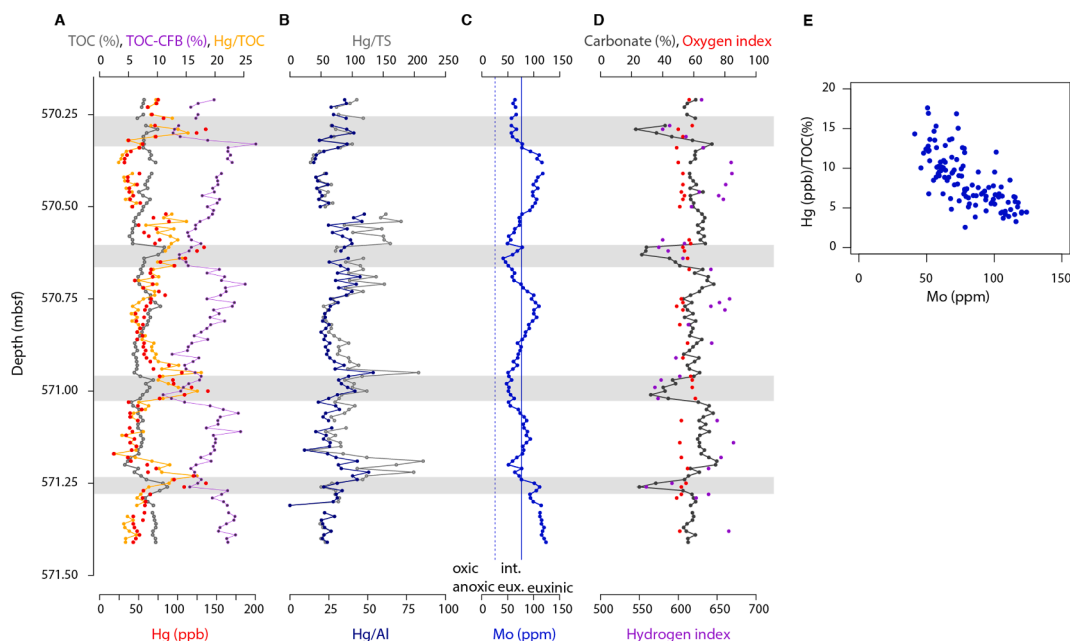
Fig. 7. Coniacian–Santonian anoxic–euxinic cyclic succession analyzed from ODP Site 1261A. A. Hg, TOC, Hg/TOC and carbonate-free (CFB) TOC. B. Al and TS-normalized Hg. C. Molybdenum (Mo) contents in ppm. D. Carbonate (%), HI and OI from Rock-Eval. Grey shaded bands indicate where März et al., (2008) inferred anoxic non-sulfidic conditions based on trace element and Fe-speciation data, abbreviation: int. eux. = intermittently euxinic. E. Hg/TOC vs Mo contents.
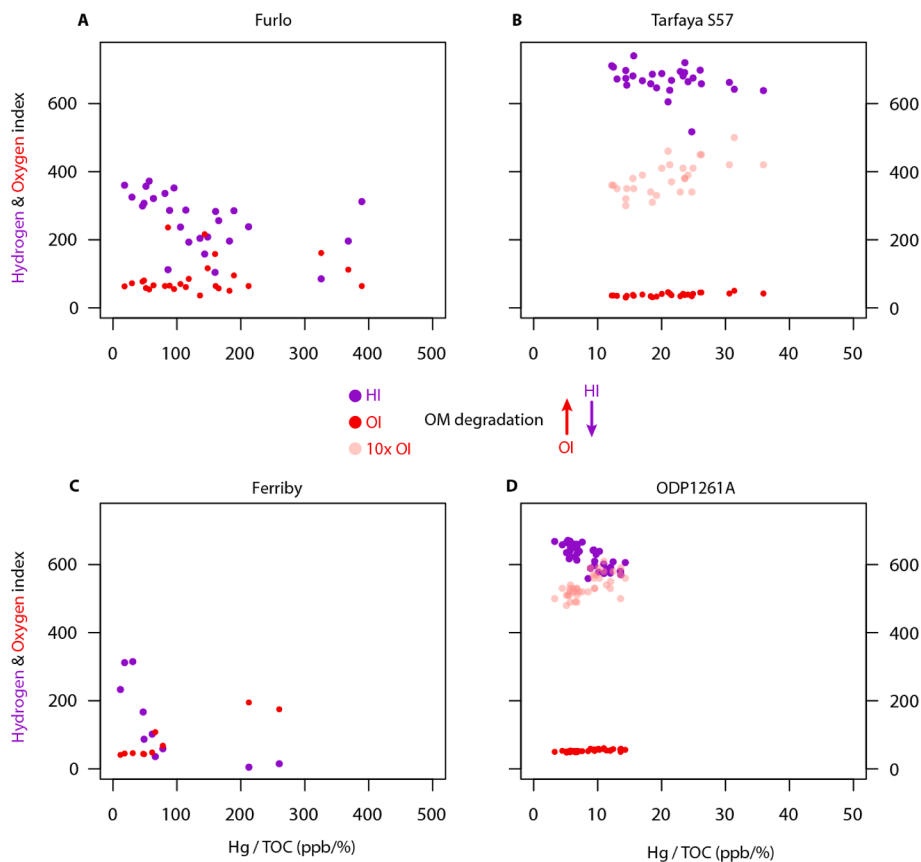

Fig. 8. Hg/TOC plotted against hydrogen and oxygen indices, illustrating the influence of organic-matter preservation state. **A.** Furlo: HI and OI vs Hg/TOC, **B.** Same for Tarfaya S57, **C.** South Ferriby and **D.** ODP Site 1261A. Note the factor of 10 Hg/TOC scale difference between panels A, C and B, D and that for panels B and D, OI is also given inflated by a factor 10 to illustrate variability.

4. Discussion

4.1. Hg and Hg/TOC trends with (de)oxygenation

4.1.1. Influence of oxic to anoxic conditions: different starting conditions, different outcome?

The Holocene Arabian Sea sediments provide insight into the effects of exposure to a range of oxygen concentrations and progressive OM breakdown on time-scales that cannot be (easily) observed in controlled environments (10 s–1000 s of years). We find only relatively minor differences in absolute Hg contents between the OMZ and more oxygenated sites (Fig. 3), especially below ~10 cm core depth. Intriguingly, the anoxic site (Station 1B, Fig. 3) has higher Hg contents at the top of the core that stabilize at a much reduced level in the lower part of the core. While this Hg trend appears to be similar to the widely documented anthropogenic contamination, the combination of the sediment age and chemical signatures of this and nearby sediment cores imply it is difficult to explain the signal with anthropogenic Hg loading (see section 3.1). Rather, we here consider the scenario that down-core Hg decrease at Station 1B hints at disproportionate Hg loss during sediment accumulation.

For the anoxic Station 1B (Fig. 3A) we can assume that Hg and TOC arrived at the sea floor in a condition that is closely representative of the export particle flux from the anoxic waters below the photic zone, with only minor alteration due to very short (~1 year) residence time in oxidizing conditions (Lengger et al., 2014). This supposition is supported by TOC contents at the anoxic site (6.5–7.5 wt%) that do not appear to differ much from the organic-carbon fraction in the export particle flux (~8 wt%) (Honjo et al., 1999). Even if only a small fraction of OM appears to be broken down, this fraction seems to contain a large proportion of the total Hg, or it may imply a significant portion of Hg deposited under these anoxic conditions is only weakly bound at time of deposition and/or can be released without noticeable changes to TOC.

The available primary and export productivity estimates across the region suggest all these stations started from a similar particle flux composition (Haake et al., 1993; Honjo et al., 1999; NASA Ocean Biology (OB.DAAC), 2014) and, without oxidation, should record similar TOC to that is observed in the particle flux and Station 1B (6.5–8%). Assuming these equal starting conditions, we calculate that a significant fraction (80–90%) of organic carbon has been lost at Stations 6B and 10, which now average only 1.2 and 0.6 wt% TOC, respectively (Fig. 3C, E). The loss of organic carbon is, however, not clearly reflected in further decreasing Hg contents compared to Station 1B. The absolute Hg content at the intermediate water depth Station 6B (Fig. 3C) is approximately half that of the stratigraphically lowermost sediments at the anoxic Station 1B (Fig. 3A), while the deep-water, well-ventilated Station 10 (Fig. 3E) shows contents similar to those found at the anoxic Station 1B (Fig. 3). The stabilized profiles of Hg and TOC suggest that the lower intervals (10–20 cm depth) of all three Arabian Sea cores represent signals that are potentially stored in the geological record.

4.1.2. Effects of local (transient) changes in oxygenation

Complementing the data from the Arabian Sea sediments, the Baltic Sea and Mediterranean sites allow us to test whether the observed trends hold for single localities experiencing different oxygenation regimes, which is situationally more similar to the geological record. These sites may also help reveal the potential influence of euxinic conditions and sulfate reduction in bottom and pore waters, which are generally considered to be negligible in the Arabian Sea (Kraal et al., 2012). In addition, the Mediterranean sapropel S1 records strong post-depositional OM oxidation ('burn-down') and influence of halted redox fronts, whereas the extremely high sediment and organic-matter accumulation rates in the Baltic Sea sites largely prevent oxygen penetration into the sediments, stifling aerobic organic-matter breakdown even during relatively well-ventilated bottom-water conditions.

Overall, the various Holocene and upper Pleistocene cores provide data sets comparable to those typically generated on core and outcrop material that records ancient (de)oxygenation events (e.g., Turgeon and Brumsack, 2006; Jenkyns, 2010). Here, we generally find low to moderate (10–100 ppb) Hg contents, which are strongly correlated with TOC, suggesting that sedimentary Hg is predominantly TOC-bound. However, some caution is warranted because sedimentary sulfur is also strongly correlated with Hg and TOC and the presence of a considerable sulfide S-associated Hg fraction might only be revealed through Hg-speciation analyses. Importantly, based on correlation with TOC, the organic-matter flux in the Baltic Sea cores controls the Hg burial flux despite very high sedimentary, organic-matter and sulfide (TS > TOC) accumulation rates. This also implies Hg availability is unlikely to have been a limiting factor in Hg drawdown efficiency in the material we examined, and, by extension, most of the ancient sediment samples analyzed to date.

When looking in more detail, we find that, despite the strong Hg–TOC and Hg–TS correlations, the Hg increase in the anoxic and sulfidic intervals in the Baltic and Mediterranean Sea cores does not entirely match the TOC or TS increases, resulting in lowered Hg/TOC at high TOC contents (Figs. 4, 5) and a similar effect can be seen in Hg/TS (Supplementary Data). Published data from Holocene–upper Pleistocene oxic–anoxic marine localities, the Japan Sea and Peruvian Margin (Shen et al., 2020), show similarly lowered Hg/TOC in sediments deposited under anoxic and euxinic conditions. However, on the strongly sulfidic end of the spectrum, the Baltic Sea core material shows the Hg/TOC–Mo correlation becomes rather insensitive at high Mo contents (Fig. 4E,F), which suggests a breakdown of the relationship during the most sulfidic episodes. This feature of the geochemistry appears consistent with the observation that, for strongly pyritized sediments (Shen et al., 2020), the relationship of Hg/TOC with low-oxygen and especially sulfidic conditions may be reversed, and may be marked by higher Hg, either as HgS or Hg inclusions in pyrite (Figs. 4, 5), commonly assumed to reflect a shift from TOC-bound to S-bound Hg deposition. However, previous studies (Shen et al., 2020) showed that TS-associations are also rare in sub-recent sediments deposited under strongly sulfidic conditions that, paired with the observation of Hg associated with diagenetic pyrite, hints at a mechanism where Hg may be (re)captured into pyrite during (late stage) diagenesis.

Furthermore, the Mediterranean sapropel record we generated confirms the occurrence of Hg focusing near paleo-redox fronts and shows, in specific cases, Hg/TOC, but notably also the Hg content itself to be elevated as a result of oxidation and/or immobilization at the oxic-anoxic boundary. This observation confirms the findings of Mercone et al. (1999), who documented large Hg spikes associated with paleo-redox fronts in oxidized sapropels and turbidites, which were hypothesized to be associated with Fe-Mn (oxyhydr)oxide scavenging. The occurrence of an ash layer at the top of sapropel S5 in some parts of the Eastern Mediterranean (a crypto tephra in core 64PE406-E1) may be argued to have added extraneous Hg in the analyzed interval. However, we consider a dominant volcanic source for this Hg spike unlikely or highly fortuitous: it remains extremely challenging to connect individual eruptions, and non-LIP activity in general, to Hg emissions (e.g. Schuster et al., 2002; Guédron et al., 2019; Edwards et al., 2021). Perhaps more importantly, the placing of the S5 Hg spike coincides exactly with the position where burn-down stopped (paleo-redox front) in sapropel S1 (Fig. 5), akin to previously studied turbidites and S1 in other Mediterranean cores (Mercone et al. 1999) where tephras are not recorded. Collectively, these data provide strong support for the findings of Mercone et al. (1999) who hypothesized that Hg released during oxidation of OM and pyrite may be focused around halted redox fronts.

The low overall Hg/TOC values observed in the Holocene anoxic Baltic Sea (Fig. 4), Holocene–upper Pleistocene sapropels (Fig. 5), Peruvian Margin sediments (Shen et al., 2020), and the anoxic Arabian Sea site are noteworthy, especially considering various inter-site differences. The Holocene data presented here from the Baltic and Arabian Sea, with Holocene-upper Pleistocene sapropel data, in concert with

published data from similar environments (Shen et al., 2020), show that shorter oxygen exposure can result in decreased Hg/TOC, through preferentially enhanced preservation of organic matter, inefficient Hg burial and likely loss of Hg. Critically, we also find, based on our data from Mediterranean sapropels and published data (e.g. Mercone et al., 1999; Shen et al., 2020), that these relationships may reverse in (1) the most oxygen-depleted, strongly sulfidic conditions that can directly (re) capture Hg in pyrite or as HgS and (2) in cases where post-depositional oxidation affects sediments deposited in anoxic–sulfidic conditions. Evidently, this process complicates the interpretation of deep-time Hg and TOC- and TS-normalized records, especially those for which no accurate, paired, oxygenation reconstructions exist.

4.1.3. Transfer of soft-sediment signals into the geological record

The material from ODP Site 1261A recovered from Demerara Rise records clear cyclic variability in sedimentary geochemistry, including Hg, during the Coniacian–Santonian Ocean Anoxic Event 3. This variability confirms that the effects documented for soft sediments are also preserved in the geological record. With deposition alternating from euxinic to ferruginous (März et al., 2008), this sedimentary material was deposited under redox conditions rather similar to the Holocene Baltic Sea sites. The organic-matter content is very high throughout (5–15%; Fig. 7) and the correlation between Hg and TOC is weak, as is the correlation of Hg with S (both $R^2 \sim 0.05$). Both Hg and TOC show cyclicity, but these cycles are not aligned or in anti-phase, implying other factors than organic-matter flux determined Hg content.

When normalizing Hg to TOC, however, clearer trends with other geochemical proxies start to appear. The sediments contain relatively minor amounts of pyrite (März et al., 2008), also evidenced by low and relatively stable TS/TOC ratios (average 0.23 ± 0.02, $n = 117$). Therefore, Hg/TS shows virtually identical trends to Hg/TOC (Fig. 7A, B). These relationships also imply that it is unlikely that a large proportion of Hg is metal sulfide-bound or present as HgS inclusions. Instead, the negative correlation of Hg/TOC with HI might imply a mechanism whereby the OM preservation state, in this case the extent of oxidative degradation, controls the Hg/TOC. Counter-intuitively, the most carbonate-lean ("black" shale) intervals have the lowest HI and highest OI in this section, which may be explained by reduced accumulation rates. Together with the stable carbonate-free Al fraction, the low HI and high OI suggest lowered accumulation rates and, as a consequence, slow, protracted, breakdown of sedimentary OM during the deposition of the carbonate-poor intervals. The behavior of Hg relative to conservative detrital elements such as Al across the oxygenation cycles mimics that of Hg/TOC and Hg/TS. This parallelism provides further support for the notion that the highest Hg preservation efficiency and perhaps accumulation rates occurred during the ferruginous phases.

Combined with the evidence for alteration of Hg and TOC signals in our Holocene core material, it seems likely that Hg and Hg/TOC signals were mostly fixed during early sedimentary diagenesis with a substantial influence of water-column and pore-water oxygenation, particularly through OM degradation in oxic settings and inefficient Hg burial and loss in anoxic settings. The observation that TOC is lost relative to Hg aligns with observations on modern organic-rich substrates such as peats and varved lake sediments (e.g., Biester et al., 2003; Rydberg et al., 2008).

The effects of ambient redox conditions, as illustrated by organic-matter preservation, also appear to be a common feature in all Cretaceous sites we studied. For example, when focusing on the Hg and TOC of the shale and chert levels at Furlo (Fig. S5), we find a positive correlation between Hg and TOC, but a weak negative correlation between Hg/TOC and HI (Fig. 8A). A negative correlation between Hg/TOC and HI and positive correlation between Hg/TOC and OI is seen at Tarfaya S57 (Fig. 8B), South Ferriby and ODP Hole 1261A (Fig. 8C,D). It is noteworthy that HI at both Furlo and South Ferriby is generally low compared to Tarfaya S57 and ODP Site 1261A (Fig. 8), and OI is generally higher, although both parameters show substantial variability,

signaling a larger contribution of refractory and generally more degraded organic matter. In this light, the higher average and more variable Hg/TOC observed at Furlo and South Ferriby is in line with previous observations, indicating a primary control of OM preservation and type on Hg/TOC, at least within single stratigraphic records, but potentially also controlling differences between time-equivalent successions.

4.2. Origin and magnitude of biases in Hg and Hg/TOC

Our new data reaffirm the observations on modern sediment that inefficient Hg burial and possibly Hg loss occurs ubiquitously under anoxic and weakly sulfidic conditions (see Section 4.1) and, most importantly, that a signal of this process might be preserved in deep-time records (e.g. Fig. 7). Such a process is an important consideration for Hg studies that attempted to constrain volcanic activity during periods of extensive anoxia such as the Mesozoic OAEs (e.g., Percival et al., 2015; Scaife et al., 2017; Percival et al., 2021b), or similar Paleozoic events (e.g., Pisarzowska et al., 2020; Rakociński et al., 2022), but also more regional or local deoxygenation, as recognized during the Cenozoic (e.g., Jones et al., 2019; Cramwinckel et al., 2022). The lowered Hg/TOC also provides some constraints on a fraction of Hg that would have been buried with the same amount of TOC assuming stable Hg/TOC, a "Hg deficit" relative to more oxygenated conditions.

Although we stress that a true Hg deficit is difficult to quantify properly without knowledge of the initial contents in the particle or burial flux, we perform a rough calculation for the Arabian Sea, assuming (1) a situation in which Hg flux to the sediment–water interface is constant and (2) a situation in which the upper part of the Station 1B sediments is representative of the original Hg/TOC ($\sim$20 ppb/%) ratio in the particle flux. Lower TOC ($\sim$8 $> \sim$6%) in the upper part of the section at Station 1B suggests that this part may have been deposited under slightly less reducing conditions or documents lower productivity compared to the lower part (Fig. 3). Even without correcting for better ventilation and lowered TOC (situation 1), the difference in Hg contents from top to bottom is substantial (Hg decreasing by 50% from $\sim$130 ppb near the sediment–water interface to 65 ppb below 10 cm depth, at Station 1B). However, assuming the Hg/TOC in the upper part is most representative of the particle flux (situation 2), the initial Hg contents in the lower part of the Station 1B core might have been even higher (up to *ca.* 170 ppb). As a consequence, we speculate that an even larger proportion of Hg ($>$60%) could have been removed during early diagenesis. While such Hg loss would not eliminate most Hg signals interpreted to result from LIP volcanism (see e.g. Grasby et al., 2019; Charbonnier et al., 2020 for a comparison of magnitudes), it appears likely that some pulses of LIP-derived Hg emitted during periods of anoxia are missed or systematically underestimated as a consequence.

We perform a similar calculation for the OAE 3 sediments, for which we calculate the Hg deficit during the sulfidic episodes relative to the ferruginous phases. Assuming the highest Hg/TOC values represent the signal without the imprint of deoxygenation effects (around 15 ppb / %), the Hg deficit for the samples with lowest Hg/TOC is $\sim$65%. For the pre-industrial, unpolluted Baltic Sea sediments, we can use the Hg/TOC from the less reducing (stable) background (Fig. 4A, C). The calculated relative Hg loss in these sediments ranges up to $\sim$40 ppb, while only $\sim$20–30 ppb is measured (up to 65% deficit). Intriguingly, while starting from different background Hg/TOC (6.4 at F80 vs 8.6 ppb/% at LL19, owing to the better ventilated nature of LL19), the calculated Hg deficit (in ppb and %) for both cores is very similar.

Remarkably, despite these uncertainties, and age and other inter-site differences between the Holocene Arabian Sea and Baltic sites and the Cretaceous ODP Hole 1261A sediments, the calculated maximum Hg deficit is very similar and typically does not exceed 65% of the total. Whether this effect originates from relatively inefficient Hg scavenging at higher TOC, or represents Hg loss during early diagenesis, as suggested by the Arabian Sea St. 1B data, is more uncertain. If the sediment

and organic-matter accumulation rates have impacted Hg scavenging efficiency through dilution (i.e., Hg supply becomes limiting), we may expect the highest accumulation rates (Baltic Sea) to show a greater Hg deficit than other successions marked by order-of-magnitude lower sediment accumulation rates (Arabian Sea and Site 1261A, Table 1a, 1b). However, the maximum Hg deficit (in %) appears remarkably similar for all these localities. Paired with the Arabian Sea data, these observations appear more consistent with partial Hg loss from sediments as a result of early diagenetic processes, than with dilution-effects that have the same expression in Hg/TOC.

When considering partial Hg loss, a maximum Hg deficit of *ca.* 65% for anoxic–mildly euxinic deposition could imply that the processes involved cannot easily (re)mobilize the remaining Hg: perhaps for this fraction the Hg-species or (binding) location inhibits remobilization. We find a strong correlation of Hg deficit to Mo enrichment and other metals that are assumed to (co)precipitate with sulfides under anoxic conditions, including the Arabian Sea station where the concentration of sulfide is very low. This result also seems to argue against a strong tendency to develop sulfide-enriched Hg or otherwise S-dominant Hg sequestration under anoxic to mildly sulfidic conditions. We find no indications that Hg is preferentially lost from or concentrated in sediments marked by continuous slightly hypoxic and oxic conditions.

The effects of oxygenation on Hg/TOC are even more pronounced compared to Hg. For the Arabian Sea sites, and other sediments deposited within and below OMZs in the ocean, the TOC contents alone may span orders of magnitude depending on the bottom- and pore-water oxygenation at the time of sediment deposition (e.g., Müller and Suess, 1979; Hartnett et al., 1998). This signal subsequently modulates Hg/TOC. Order-of-magnitude changes, such as we find in the Arabian Sea sites, do not commonly occur in one single succession because most analyzed depositional settings will not have changed so dramatically. However, both the Baltic Sea and ODP Site 1261 stratigraphic records clearly show changes to Hg and Hg/TOC related to redox changes (Figs. 4, 6). Hence, extreme caution should be taken when analyzing successions across (de)oxygenation events, since signal amplification or suppression in Hg/TOC is likely to have occurred and can span at least an order of magnitude, on a par with many of the inferred volcanism-related Hg/TOC fluctuations in the geological record (Charbonnier et al., 2020). Likewise, the oxidation biases may have induced changes that exceed the commonly used limit for interpreting Hg enrichment factors (HgEF > 2 Shen et al., 2019a, 2019b; Zhu et al., 2021). A more conservative approach is therefore warranted when interpreting Hg/TOC or otherwise-normalized Hg records and perhaps even raw Hg data and could, for example, utilize a series of criteria. The observations on the potential impact of ambient redox conditions on Hg and normalized Hg may warrant revisiting of Hg studies that are based on successions where substantial changes in ambient redox were recognized (e.g. Percival et al., 2018; Jones et al., 2019; Paschall et al., 2019; Rakociński et al., 2021; Bian et al., 2022; Zhao et al., 2022)). Crucially, we find that any anomalously elevated Hg/TOC data should at least be accompanied by substantially (at least > 3 fold background) elevated Hg (as suggested previously; Percival et al., 2021) and, as such spikes might be associated with post-depositional oxidation of anoxic facies, evidence for stable redox conditions in the relevant stratigraphic interval that would support increased primary Hg loading.

4.3. Processes influencing Hg and Hg/TOC during early diagenesis

In our new data (Figs. 3–8) the TOC-normalized Hg (i.e., Hg/TOC) unambiguously increases with oxidation although this effect seems to result from multiple distinct processes affecting Hg and TOC separately. Specifically, there appears to be a distinction in Hg burial efficiency between oxygenated and anoxic to sulfidic conditions, whereby Hg may experience inefficient scavenging or preferentially escape sediments under anoxic to sulfidic conditions while there is no measurable change in TOC content of the sediment (see Sections 4.1 and 4.2). The similar

maximum Hg deficit between sites might signal that a certain part of the Hg cannot be easily mobilized with processes that typically take place under anoxic and mildly sulfidic conditions. For example, it has been established that certain inorganic Hg species (HgS, dissolved Hg^{2+}) appear relatively inaccessible to microbial Hg cycling, whereas the same may not apply for organic Hg species (e.g. Mazrui et al., 2016; Zhu et al., 2018). It might also be that redox conditions are preventing further Hg loss through supplying sulfide to (re)sequester Hg (as HgS or within pyrite) or that sulfate- and iron-reducing microbiota responsible for Hg cycling are limited by sulfide concentrations (Benoit et al., 1999; Hammerschmidt and Fitzgerald, 2004; Hammerschmidt et al., 2008). In contrast to organic-matter dilution, these options require partial Hg remobilization after initial scavenging in the water column or from sediments, whereby ultimately up to *ca.* 50–65% less Hg (see Section 4.2) is buried. Below we explore processes that may result in preferential Hg loss, with the proviso that we do not exclude the possibility that OM-dilution effects also shape Hg/TOC.

Due to a general lack of geological data on Hg speciation, we cannot identify which phases are most actively involved in sedimentary Hg cycling, or confirm the occurrence of a specific process leading to Hg loss in anoxic to sulfidic environments, in which loss of organic matter would be minimal. There are, however, potential explanations for the slowly decreasing Hg contents in the intervals of Fe-reduction (and SO_4^{2-} reduction, see 2.1) in the anoxic Holocene sediments of the Arabian Sea (Fig. 3) and the lower Hg loading of TOC in the organic-rich, sulfidic, Holocene sediments of the Baltic Sea (Fig. 4). For example, it has been established that various sulfate- and Fe-reducing bacteria and archaea are able to methylate Hg to counteract its toxicity (Fleming et al., 2006; Gilmour et al., 2013). This distinct microbial behavior, also known from other biotoxic elements (Li et al., 2021), and net release of MeHg to the water column has been recognized in marine sediments (e.g. Mason et al., 2006). Optimum Hg methylation rates were found to be around 1 μM sulfide in natural environments (Mason et al., 2006) although spatial variability due to differences in microbial communities are likely (King et al., 2001). While a direct flux of MeHg from sediments may not appreciably increase Hg mobility, the more volatile dimethylmercury (DMHg) may form from MeHg in the presence of sulfide (Craig and Moreton, 1984; Jonsson et al., 2016). Another pathway for further dispersal of Hg from MeHg occurs through (anaerobic) reduction of MeHg and subsequent Hg^0 formation (Mason et al., 1995; Yu et al., 2012). Finally, (a)biotic reduction pathways of Hg^{2+} may lead to Hg^0 formation directly and play a major role in upper water-column Hg cycling (Soerensen et al., 2010) but likely also occur below the photic zone (Poulain et al., 2004; Kritee et al., 2007). The geological relevance of all these processes remains unknown.

While it is impossible to confidently identify the process responsible for removal of Hg, our data appear consistent with a mechanism whereby Hg methylation or other Hg reduction processes facilitate Hg loss. Specifically, the negative correlation of Hg/TOC, and notably Hg/Al, with elevated Mo contents, which is used as evidence for sulfidic (pore-water) conditions at the time of deposition at ODP Site 1261, is interesting and mimics the trends observed in the Baltic Sea sites. Because sulfide is an important modulator of Mo sequestration, the negative correlation between Mo and Hg/TOC tentatively supports a role for Hg methylation by sulfate reducers in Hg loss. Intriguingly, the negative correlations between Hg/TOC and Mo weaken at high Mo contents (>50 ppm in the Baltic Sea sites, Fig. 4E, F and >100 ppm for ODP Site 1261 Fig. 7D), which may be indicative of sulfide inhibition on Hg cycling by sulfate- and iron-reducing organisms, and may be accompanied with, or followed by, a switch to Hg sequestration by sulfide or metal sulfide complexes when these species are abundantly available (Ullrich et al., 2001; Rosati et al., 2018; Shen et al., 2020). Alternatively, working either in tandem with or independently from Hg-methylation, an influence of temporary adsorption of Hg^{2+} with Fe or Mn (oxyhydr)oxide in Hg cycling cannot be ruled out. The mobility of Hg^{2+} would likely remain a limiting factor under these conditions, in the

presence of efficient scavenging ligands such as free sulfide and organic matter.

At present, it is impossible to gauge exactly how processes leading to Hg deficits or Hg loss have influenced deep-time records, but noticeable Hg deficits relative to TOC and TS occur under ferruginous–mildly euxinic conditions. A degree of Hg loss is consistent with the trends we find from the Holocene Baltic Sea sites, Pleistocene Mediterranean sapropel S5 and the Coniacian-Santonian OAE 3 sediments recovered at ODP Site 1261. Crucially, the observed Hg deficit – up to ~65% relative to stable Hg/TOC – occurs, in similar magnitude, both in deep-time and modern sediments, suggesting that this phenomenon might be a relatively common feature. Moreover, if Hg evasion is indeed a common process in low-oxygen environments, questions are raised regarding the potential for redistribution and redeposition of Hg. The redistribution may lead to enhanced Hg burial in places with strongly sulfidic conditions, or at the interface between anoxic and oxic waters. The negative correlations of Hg and Hg/TOC with Mo and other redox-sensitive elements might be useful in identifying Hg deficits. Regardless of the processes involved, the geological imprint of processes potentially leading to Hg loss from sediments warrant careful consideration when interpreting the geological Hg record.

We see progressive TOC loss with increased oxygen exposure, especially under oxic or mildly hypoxic conditions. However, Hg is not proportionally affected, resulting in progressively higher Hg/TOC with long-term oxidation, and occasionally Hg focusing (e.g., Fig. 5, Mercone et al. 1999). The early diagenetic changes examined here have echoed effects in situations where ancient sediments, initially deposited under anoxic conditions, have been subjected to surface weathering and oxidation in more recent time (Charbonnier et al., 2020). There are a couple of plausible mechanisms that would retain more Hg relative to TOC during oxidation. Firstly, if Hg were mobilized (as Hg^{2+}) during OM breakdown, even small amounts of remaining organic material, Fe/Mn (oxyhydr)oxides, pyrite and other sulfides could immediately recapture this Hg, whereas dissolved inorganic carbon would be generally more mobile. Secondly, it is likely that a fraction of the sedimentary Hg would be associated with more refractory OM (e.g., Them et al. 2019), which could have had intrinsically higher Hg/TOC and was less easily mobilized (Them et al., 2019; Charbonnier et al., 2020). A relative increase in the refractory organic-matter fraction could hence cause a steeper Hg/TOC relationship during extensive TOC degradation, whereas a relative decrease in refractory organic matter would result in flattening of the curves at higher TOC. Further detailed assessment of OM characteristics through, for example, maceral analyses or palynology, or Hg content data on specific types of OM, might help elucidate how preservation and OM sources interact to shape Hg/TOC patterns in ancient sediments. Even if some of those data types are available for some localities and periods, it is typically not paired with Hg (e.g., Harding et al., 2011; Kender et al., 2012; Jones et al., 2019; Kender et al., 2021), and these aspects are thus under-explored. Broad geochemical characteristics of OM (such as HI and OI, but also C/N ratios) might be used as first-order estimates of the preservation state (Fig. 8) as well as the relative contribution of refractory OM.

5. Conclusions

Differences in duration and intensity of sediment (de)oxygenation and, more broadly, changes in redox conditions, both between and within our Holocene–Pleistocene and Cretaceous sites resulted in markedly divergent Hg contents and Hg/TOC (Figs. 3–8). The amplitude of these changes is such that they warrant careful consideration when interpreting the geological record for paleo-volcanic activity. Importantly, we find that separate processes affect both the Hg and TOC, and contribute to the complexity and potential biases that may pose an additional challenge in the interpretation of Hg and Hg/TOC records. Through selecting sites with stable Hg loading throughout but with spatially or temporally variable ambient redox conditions and evolution,

we isolate the effects of the redox conditions on the Hg and normalized-Hg records and how those effects might be stored in the geological record.

Results from the Holocene Arabian Sea cores show that order-of-magnitude differences in Hg/TOC can occur after oxidizing seemingly similar starting material. Under oxygen-depleted conditions, there is evidence that part of the Hg escapes the sediments during initial diagenesis, for example after methylation by Fe-oxide- and sulfate-reducing bacteria and methanogens. If this phenomenon were a common factor during early diagenesis, it might be expected that Hg spikes would be suppressed in sediments deposited under such low-oxygen conditions. Such sediments are also commonly characterized by high burial efficiency of organic matter, arguably further reducing the Hg/TOC ratio. Aerobic degradation, on the other hand, seems to predominantly affect sedimentary organic carbon, while Hg is mostly retained, thereby inflating Hg/TOC ratios. Stratigraphic focusing of Hg was found associated with the oxidized intervals of sediments that were deposited under anoxic–sulfidic conditions. Under such circumstances, spikes in Hg content are observed around buried redox fronts, which are commonly associated with, but not unique to, turbidites (e.g., Mercone et al. 1999) and sapropels (Fig. 5). These types of settings, as a consequence, are particularly challenging targets for assessing paleo-volcanic activity.

For many key intervals in geological deep time that have been investigated for Hg and TOC, the potential influences of (de)oxygenation have far-reaching implications. Such complicating factors could be particularly important for periods associated with emplacement of subaerial LIPs that are also commonly associated with the most extreme carbon-cycle, climatic and environmental perturbations, including (transient) expansion of low-oxygen areas in the ocean, in extreme cases leading to oceanic anoxic events. It is noteworthy that some overwhelmingly large Hg spikes occur during times of ocean anoxia, while our results show that deoxygenation generally has a higher probability of obscuring, rather than accentuating Hg/TOC spikes (e.g. Fig. 6). Indeed, it appears that under anoxic and (mildly) euxinic conditions Hg contents may be suppressed due to Hg evasion, perhaps as a result of methylation and subsequent MeHg cycling in pore waters or in the water column (Fig. 3, 4, 6, 7). We cannot rule out the possibility that oceanic anoxia, such as occurred during the Mesozoic Era, in combination with the nature of the LIP volcanism, may have played an important role in reducing the perceived impact on the Hg cycle (e.g., Percival et al., 2018). On the other hand, high-amplitude oxygen fluctuations are likely to have led to increased variability in Hg and TOC and, in some cases, to Hg focusing resulting from oxidation of previously anoxic sediments.

It also remains likely that S-driven Hg sequestration (within pyrite) occurs in permanent and strongly euxinic conditions, potentially amplifying Hg signals, but the sedimentary host phases and their potential for amplified Hg sequestration in geological samples will remain uncertain until a broad spectrum of dedicated Hg speciation data becomes available. We also highlight the need for studies focusing on potential Hg host-phase shifts during diagenesis and especially paired Hg and S behavior during alteration of the TOC and sulfur pools (sulfurization and diagenetic pyrite formation). Lastly, the geological record of MeHg remains largely untested but may allow unique insights into how Hg is sequestered if major outstanding unknowns surrounding preservation and processes contributing to methylation and demethylation in sediments on geological time-scales can be constrained.

Regardless of the contributing processes, the magnitude of geochemical change from early diagenesis to both the Hg and TOC records is such that the resulting signals, without prior knowledge of the oxygenation history of a succession, could easily be misinterpreted as evidence for enhanced, suppressed, or intermittent volcanic activity. While the relative influence of oxygenation on any single record during high-amplitude environmental changes remains difficult to quantify, we calculate Hg deficits up to 65% in multiple records, while changes associated with Hg focusing around paleo-redox fronts is potentially of a

similar magnitude (~a doubling). Critically, we also show that Hg/TOC might suffer order-of-magnitude alterations depending on the oxidative evolution of the host sediment. As such, we recommend paleo-oxygenation reconstructions through, for example, the use of (trace)-element analyses or, more indirectly, organic-matter characteristics, be employed as extensively as possible when interpreting Hg and (TOC-) normalized Hg signals.

Declaration of Competing Interest

The authors declare that they have no known competing financial interests or personal relationships that could have appeared to influence the work reported in this paper.

Acknowledgments

Appendix A. Supplementary material

The supplementary materials contain a more detailed description of each of the investigated sites (section 1) and a detailed description of the results obtained from the Furlo locality (Italy) (section 2). Figures included in the supplementary material show mercury *versus* total organic carbon or total sulfur for the Arabian Sea cores used in this work (Figure S1), the Baltic Sea material (2), ODP Hole 1261A (3), Tarfaya core S57 and South Ferriby (4) and Furlo (5). All data that were generated for this study or used in figures are available as supplementary data tables Supplementary material to this article can be found online at https://doi.org/10.1016/j.gca.2023.04.015.

References

Amos, H.M., Jacob, D.J., Streets, D.G., Sunderland, E.M., 2013. Legacy impacts of all-time anthropogenic emissions on the global mercury cycle. Global Biogeochem. Cycles 27, 410–421.

Amos, H.M., Sonke, J.E., Obrist, D., Robins, N., Hagan, N., Horowitz, H.M., Mason, R.P., Witt, M., Hedgecock, I.M., Corbitt, E.S., Sunderland, E.M., 2015. Observational and modeling constraints on global anthropogenic enrichment of mercury. Environ. Sci. Technol. 49, 4036–4047.

Behar, F., Beaumont, V., De, B., Penteado, H.L., 2001. Rock-Eval 6 technology: performances and developments. Oil Gas Sci. Technol. 56, 111–134.

Benoit, J.M., Gilmour, C.C., Mason, R.P., Heyes, A., 1999. Sulfide controls on mercury speciation and bioavailability to methylating bacteria in sediment pore waters. Environ. Sci. Technol. 33, 951–957.

Berner, R.A., 1984. Sedimentary pyrite formation: An update. Geochim. Cosmochim. Acta 48, 605–615.

Bian, L., Chappaz, A., Schovsbo, N.H., Nielsen, A.T., Sanei, H., 2022. High mercury enrichments in sediments from the Baltic continent across the late Cambrian: Controls and implications. Chem. Geol. 599, 120846.

Biester, H., Martinez-Cortizas, A., Birkenstock, S., Kilian, R., 2003. Effect of peat decomposition and mass loss on historic mercury records in peat bogs from patagonia. Environ. Sci. Technol. 37, 32–39.

Biester, H., Pérez-Rodríguez, M., Gilfedder, B.-S., Martínez, C.A., Hermanns, Y.-M., 2018. Solar irradiance and primary productivity controlled mercury accumulation in sediments of a remote lake in the Southern Hemisphere during the past 4000 years. Limnol. Oceanogr. 63, 540–549.

Bowman, K.L., Hammerschmidt, C.R., Lamborg, C.H., Swarr, G., 2015. Mercury in the North Atlantic Ocean: The U.S. GEOTRACES zonal and meridional sections. Deep Sea Res. Part II Top. Stud. Oceanogr. 116, 251–261.

Bowman, K.L., Hammerschmidt, C.R., Lamborg, C.H., Swarr, G.J., Agather, A.M., 2016. Distribution of mercury species across a zonal section of the eastern tropical South Pacific Ocean (U.S. GEOTRACES GP16). Mar. Chem. 186, 156–166.

Brumsack, H.J., 2006. The trace metal content of recent organic carbon-rich sediments: Implications for Cretaceous black shale formation. Palaeogeogr. Palaeoclimatol. Palaeoecol. 232, 344–361.

Charbonnier, G., Adatte, T., Föllmi, K.B., Suan, G., 2020. Effect of intense weathering and postdepositional degradation of organic matter on Hg/TOC proxy in organic-rich sediments and its implicationsfor deep-time investigations. Geochem. Geophys. Geosyst. 21, e2019GC008707.

Clarkson, M.O., Stirling, C.H., Jenkyns, H.C., Dickson, A.J., Porcelli, D., Moy, C.M., von Strandmann, P.A.E., Cooke, I.R., Lenton, T.M., 2018. Uranium isotope evidence for two episodes of deoxygenation during Oceanic Anoxic Event 2. Proc. Natl. Acad. Sci. U. S. A. 115, 2918–2923.

Clarkson, M.O., Hennekam, R., Sweere, T.C., Andersen, M.B., Reichart, G.J., Vance, D., 2021. Carbonate associated uranium isotopes as a novel local redox indicator in oxidatively disturbed reducing sediments. Geochim. Cosmochim. Acta 311, 12–28.

Cohen, A.S., Coe, A.L., Harding, S.M., Schwark, L., 2004. Osmium isotope evidence for the regulation of atmospheric CO$_2$ by continental weathering. Geology 32, 157–160.

Cossa, D., Knoery, J., Bănaru, D., Harmelin-Vivien, M., Sonke, J.E., Hedgecock, I.M., Bravo, A.G., Rosati, G., Canu, D., Horvat, M., Sprovieri, F., Pirrone, N., Heimbürger-Boavida, L.-E., 2022. Mediterranean Mercury Assessment 2022: An updated budget, health consequences, and research perspectives. Environ. Sci. Technol. 56, 3840–3862.

Covelli, S., Faganeli, J., Horvat, M., Brambati, A., 2001. Mercury contamination of coastal sediments as the result of long-term cinnabar mining activity (Gulf of Trieste, northern Adriatic sea). Appl. Geochem. 16, 541–558.

Craig, P.J., Moreton, P.A., 1984. The role of sulphide in the formation of dimethyl mercury in river and estuary sediments. Mar. Pollut. Bull. 15, 406–408.

Cramwinckel, M.J., van der Ploeg, R., van Helmond, N.A.G.M., Waarlo, N., Agnini, C., Bijl, P.K., van der Boon, A., Brinkhuis, H., Frieling, J., Krijgsman, W., Mather, T.A., Middelburg, J.J., Peterse, F., Slomp, C.P., Sluijs, A., 2022. Deoxygenation and organic carbon sequestration in the Tethyan realm associated with the Middle Eocene Climatic Optimum. GSA Bull. 135, 1280–1296.

Dal Corso, J., Mills, B.J.W., Chu, D., Newton, R.J., Mather, T.A., Shu, W., Wu, Y., Tong, J., Wignall, P.B., 2020. Permo-Triassic boundary carbon and mercury cycling linked to terrestrial ecosystem collapse. Nat. Commun. 11, 2962.

Du Vivier, A.D.C., Selby, D., Sageman, B.B., Jarvis, I., Gröcke, D.R., Voigt, S., 2014. Marine 187Os/188Os isotope stratigraphy reveals the interaction of volcanism and ocean circulation during Oceanic Anoxic Event 2. Earth Planet. Sci. Lett. 389, 23–33.

Edwards, B.A., Kushner, D.S., Outridge, P.M., Wang, F., 2021. Fifty years of volcanic mercury emission research: Knowledge gaps and future directions. Sci. Total Environ. 757, 1–17.

Ernst, R.E., Youbi, N., 2017. How Large Igneous Provinces affect global climate, sometimes cause mass extinctions, and represent natural markers in the geological record. Palaeogeogr. Palaeoclimatol. Palaeoecol. 478, 30–52.

Fendley, I.M., Mittal, T., Sprain, C.J., Marvin-DiPasquale, M., Tobin, T.S., Renne, P.R., 2019. Constraints on the volume and rate of Deccan Traps flood basalt eruptions using a combination of high-resolution terrestrial mercury records and geochemical box models. Earth Planet. Sci. Lett. 524, 1–11.

Fitzgerald, W.F., Lamborg, C.H., Hammerschmidt, C.R., 2007. Marine biogeochemical cycling of mercury. Chem. Rev. 107, 641–662.

Fleming, E.J., Mack, E.E., Green, P.G., Nelson, D.C., 2006. Mercury methylation from unexpected sources: Molybdate-inhibited freshwater sediments and an iron-reducing bacterium. Appl. Environ. Microbiol. 72, 457–464.

Gagnon, C., Pelletier, É., Mucci, A., 1997. Behaviour of anthropogenic mercury in coastal marine sediments. Mar. Chem. 59, 159–176.

Gehrke, G.E., Blum, J.D., Meyers, P.A., 2009. The geochemical behavior and isotopic composition of Hg in a mid-Pleistocene western Mediterranean sapropel. Geochim. Cosmochim. Acta 73, 1651–1665.

Gilmour, C.C., Podar, M., Bullock, A.L., Graham, A.M., Brown, S.D., Somenahally, A.C., Johs, A., Hurt, R.A., Bailey, K.L., Elias, D.A., 2013. Mercury methylation by novel microorganisms from new environments. Environ. Sci. Technol. 47, 11810–11820.

Grasby, S.E., Sanei, H., Beauchamp, B., Chen, Z., 2013. Mercury deposition through the Permo-Triassic Biotic Crisis. Chem. Geol. 351, 209–216.

Grasby, S.E., Them, T.R., Chen, Z., Yin, R., Ardakani, O.H., 2019. Mercury as a proxy for volcanic emissions in the geologic record. Earth-Science Rev. 196, 102880.

Guédron, S., Tolu, J., Brisset, E., Sabatier, P., Perrot, V., Bouchet, S., Develle, A.L., Bindler, R., Cossa, D., Fritz, S.C., Baker, P.A., 2019. Late Holocene volcanic and anthropogenic mercury deposition in the western Central Andes (Lake Chungará Chile). Sci. Total Environ. 662, 903–914.

Haake, B., Ittekkot, V., Rixen, T., Ramaswamy, V., Nair, R.R., Curry, W.B., 1993. Seasonality and interannual variability of particle fluxes to the deep Arabian sea. Deep Sea Res. Part I 40, 1323–1344.

Hammerschmidt, C.R., Fitzgerald, W.F., 2004. Geochemical controls on the production and distribution of methylmercury in near-shore marine sediments. Environ. Sci. Technol. 38, 1487–1495.

Hammerschmidt, C.R., Fitzgerald, W.F., Balcom, P.H., Visscher, P.T., 2008. Organic matter and sulfide inhibit methylmercury production in sediments of New York/New Jersey Harbor. Mar. Chem. 109, 165–182.

Harding, I.C., Charles, A.J., Marshall, J.E.A., Pälike, H., Roberts, A.P., Wilson, P.A., Jarvis, E., Thorne, R., Morris, E., Moremon, R., Pearce, R.B., Akbari, S., 2011. Sea-level and salinity fluctuations during the Paleocene-Eocene thermal maximum in Arctic Spitsbergen. Earth Planet. Sci. Lett. 303, 97–107.

Hartnett, H.E., Keil, R.G., Hedges, J.I., Devol, A.H., 1998. Influenceof oxygen exposure time on organic carbon preservation in continental margin sediments. Nature 391, 572–574.

Hazra, B., Katz, B.J., Pratap, D., Singh, P.K., 2022. Impact of siderite on Rock-Eval S3 and oxygen index. Mar. Pet. Geol. 143, 105804.

Heimbürger, L.E., Cossa, D., Marty, J.C., Migon, C., Averty, B., Dufour, A., Ras, J., 2010. Methyl mercury distributions in relation to the presence of nano- and picophytoplankton in an oceanic water column (Ligurian Sea, North-western Mediterranean). Geochim. Cosmochim. Acta 74, 5549–5559.

Hennekam, R., van der Bolt, B., van Nes, E.H., de Lange, G.J., Scheffer, M., Reichart, G.J., 2020. Early-warning signals for marine anoxic events. Geophys. Res. Lett. 47 e2020GL089183.

Honjo, S., Dymond, J., Prell, W., Ittekkot, V., 1999. Monsoon-controlled export fluxes to the interior of the Arabian Sea. Deep Sea Res. Part II Top. Stud. Oceanogr. 46, 1859–1902.

Jenkyns, H.C., 2010. Geochemistry of oceanic anoxic events. Geochem. Geophys. Geosyst. 11, Q03004.

Jenkyns, H.C., Matthews, A., Tsikos, H., Erel, Y., 2007. Nitrate reduction, sulfate reduction, and sedimentary iron isotope evolution during the Cenomanian-Turonian oceanic anoxic event. Paleoceanography 22, PA3208.

Jilbert, T., Slomp, C.P., 2013. Rapid high-amplitude variability in Baltic Sea hypoxia during the holocene. Geology 41, 1183–1186.

Jones, M.T., Percival, L.M.E., Stokke, E.W., Frieling, J., Mather, T.A., Riber, L., Schubert, B.A., Schultz, B., Tegner, C., Planke, S., Svensen, H.H., 2019. Mercury anomalies across the Palaeocene-Eocene Thermal Maximum. Clim. Past 15, 217–236.

Jonsson, S., Mazrui, N.M., Mason, R.P., 2016. Dimethylmercury formation mediated by inorganic and organic reduced sulfur surfaces. Sci. Rep. 6, 27958.

Kender, S., Stephenson, M.H., Riding, J.B., Leng, M.J., Knox, R.W.O.B., Peck, V.L., Kendrick, C.P., Ellis, M.A., Vane, C.H., Jamieson, R., 2012. Marine and terrestrial environmental changes in NW Europe preceding carbon release at the Paleocene-Eocene transition. Earth Planet. Sci. Lett. 353–354, 108–120.

Kender, S., Bogus, K., Pedersen, G.K., Dybkjær, K., Mather, T.A., Mariani, E., Ridgwell, A., Riding, J.B., Wagner, T., Hesselbo, S.P., Leng, M.J., 2021. Paleocene/Eocene carbon feedbacks triggered by volcanic activity. Nat. Commun. 12, 5186.

King, J.K., Kostka, J.E., Frischer, M.E., Saunders, F.M., Jahnke, R.A., 2001. A Quantitative relationship that demonstrates mercury methylation rates in marine sediments are based on the community composition and activity of sulfate-reducing bacteria. Environ. Sci. Technol. 35, 2491–2496.

Koho, K.A., Nierop, K.G.J., Moodley, L., Middelburg, J.J., Pozzato, L., Soetaert, K., Van Der Plicht, J., Reichart, G.J., 2013. Microbial bioavailability regulates organic matter preservation in marine sediments. Biogeosciences 10, 1131–1141.

Kraal, P., Slomp, C.P., Reed, D.C., Reichart, G.-J., Poulton, S.W., 2012. Sedimentary phosphorus and iron cycling in and below the oxygen minimum zone of the northern Arabian Sea. Biogeosciences 9, 2603–2624.

Kritee, K., Blum, J.D., Johnson, M.W., Bergquist, B.A., Barkay, T., 2007. Mercury stable isotope fractionation during reduction of Hg(II) to Hg(0) by Mercury resistant microorganisms. Environ. Sci. Technol. 41, 1889–1895.

Lafargue, E., Marquis, F., Pillot, D., 1998. Rock-Eval 6 applications in hydrocarbon exploration, production, and soil contamination studies. Rev. l'Institut Fr. du Pet. 53, 421–437.

Leipe, T., Moros, M., Kotilainen, A., Vallius, H., Kabel, K., Endler, M., Kowalski, N., 2013. Mercury in Baltic Sea sediments-Natural background and anthropogenic impact. Chem. Erde 73, 249–259.

Lengger, S.K., Hopmans, E.C., Sinninghe Damsté, J.S., Schouten, S., 2014. Impact of sedimentary degradation and deep water column production on GDGT abundance and distribution in surface sediments in the Arabian Sea: Implications for the TEX$_{86}$ paleothermometer. Geochim. Cosmochim. Acta 142, 386–399.

Li, Y.P., Ben, F.I., Chi, F.E., Moraleda-Munoz, A., Li, X., Rosen, B.P., Yoshinaga, M., Rensing, C., 2021. Antimicrobial activity of metals and metalloids. Annu. Rev. Microbiol. 75, 175–197.

Lyons, T.W., Anbar, A.D., Severmann, S., Scott, C., Gill, B.C., 2009. Tracking euxinia in the ancient ocean: A multiproxy perspective and Proterozoic case study. Annu. Rev. Earth Planet. Sci. 37, 507–534.

Machado, W., Sanders, C.J., Santos, C.J., Sanders, I.R., Sanders, L.M., Silva-Filho, E.V., Luiz-Silva, W., 2016. Mercury dilution by autochthonous organic matter in a fertilized mangrove wetland. Environ. Pollut. 213, 30–35.

März, C., Poulton, S.W., Beckmann, B., Küster, K., Wagner, T., Kasten, S., 2008. Redox sensitivity of P cycling during marine black shale formation: Dynamics of sulfidic and anoxic, non-sulfidic bottom waters. Geochim. Cosmochim. Acta 72, 3703–3717.

Mason, R.P., Fitzgerald, W.F., Morel, F.M.M., 1994. The biogeochemical cycling of elemental mercury: Anthropogenic influences. Geochim. Cosmochim. Acta 58, 3191–3198.

Mason, R.P., Morel, F.M.M., Hemond, H.F., 1995. The role of microorganisms in elemental mercury formation in natural waters. Water, Air, Soil Pollut. 80, 775–787.

Mason, R.P., Kim, E.H., Cornwell, J., Heyes, D., 2006. An examination of the factors influencing the flux of mercury, methylmercury and other constituents from estuarine sediment. Mar. Chem. 102, 96–110.

Mason, R.P., Sheu, G.R., 2002. Role of ocean in the global mercury cycle. Global Biogeochem. Cycles 16, 1093.

Mason, R.P., Choi, A.L., Fitzgerald, W.F., Hammerschmidt, C.R., Lamborg, C.H., Soerensen, A.L., Sunderland, E.M., 2012. Mercury biogeochemical cycling in the ocean and policy implications. Environ. Res. 119, 101–117.

Mazrui, N.M., Jonsson, S., Thota, S., Zhao, J., Mason, R.P., 2016. Enhanced availability of mercury bound to dissolved organic matter for methylation in marine sediments. Geochim. Cosmochim. Acta 194, 153–162.

Mercone, D., Thomson, J., Croudace, I., Troelstra, S., 1999. A coupled natural immobilisation mechanism for mercury and selenium in deep-sea sediments. Geochim. Cosmochim. Acta 63, 1481–1488.

Mikac, N., Niessen, S., Ouddane, B., Wartel, M., 1999. Speciation of mercury in sediments of the Seine estuary (France). Appl. Organomet. Chem. 13, 715–725.

Müller, P.J., Suess, E., 1979. Productivity, sedimentation rate, and sedimentary organic matter in the oceans—I. Organic carbon preservation. Deep Sea Res. Part A. Oceanogr. Res. Pap. 26, 1347–1362.

NASA Ocean Biology (OB.DAAC), 2014. Mean annual sea surface chlorophyll-a concentration for the period 2009-2013 (composite dataset created by UNEP-WCMC).

Nieuwenhuize, J., Maas, Y.E.M., Middelburg, J.J., 1994. Rapid analysis of organic carbon and nitrogen in particulate materials. Mar. Chem. 45, 217–224.

Outridge, P.M., Sanei, H., Stern, G.A., Hamilton, P.B., Goodarzi, F., 2007. Evidence for control of mercury accumulation rates in Canadian High Arctic Lake sediments by variations of aquatic primary productivity. Environ. Sci. Technol. 41, 5259–5265.

Owens, J.D., Lyons, T.W., Hardisty, D.S., Lowery, C.M., Lu, Z., Lee, B., Jenkyns, H.C., 2017. Patterns of local and global redox variability during the Cenomanian-Turonian Boundary Event (Oceanic Anoxic Event 2) recorded in carbonates and shales from central Italy. Sedimentology 64, 168–185.

Paschall, O., Carmichael, S.K., Königshof, P., Waters, J.A., Ta, P.H., Komatsu, T., Dombrowski, A., 2019. The Devonian-Carboniferous boundary in Vietnam: Sustained ocean anoxia with a volcanic trigger for the Hangenberg Crisis? Glob. Planet. Change 175, 64–81.

Percival, L.M.E., Witt, M.L.I., Mather, T.A., Hermoso, M., Jenkyns, H.C., Hesselbo, S.P., Al-Suwaidi, A.H., Storm, M.S., Xu, W., Ruhl, M., 2015. Globally enhanced mercury deposition during the end-Pliensbachian extinction and Toarcian OAE: A link to the Karoo-Ferrar Large Igneous Province. Earth Planet. Sci. Lett. 428, 267–280.

Percival, L.M.E., Ruhl, M., Hesselbo, S.P., Jenkyns, H.C., Mather, T.A., Whiteside, J.H., 2017. Mercury evidence for pulsed volcanism during the end-Triassic mass extinction. Proc. Natl. Acad. Sci. U. S. A. 114, 7929–7934.

Percival, L.M.E., Jenkyns, H.C., Mather, T.A., Dickson, A.J., Batenburg, S.J., Ruhl, M., Hesselbo, S.P., Barclay, R., Jarvis, I., Robinson, S.A., Woelders, L., 2018. Does large igneous province volcanism always perturb the mercury cycle? Comparing the records of Oceanic Anoxic Event 2 and the end-Cretaceous to other Mesozoic events. Am. J. Sci. 318, 799–860.

Percival, L.M.E., Bergquist, B.A., Mather, T.A., Sanei, H., 2021a. Sedimentary mercury enrichments as a tracer of large igneous province volcanism. In: Ernst, R.E., Dickson, A.J., Bekker, A. (Eds.), Large Igneous Provinces: A Driver of Global Environmental and Biotic Changes. Geophysical Monograph Series, American Geophysical Union, pp. 247–262.

Percival, L.M.E., Tedeschi, L.R., Creaser, R.A., Bottini, C., Erba, E., Giraud, F., Svensen, H., Savian, J., Trindade, R., Coccioni, R., Frontalini, F., Jovane, L., Mather, T.A., Jenkyns, H.C., 2021b. Determining the style and provenance of magmatic activity during the Early Aptian Oceanic Anoxic Event (OAE 1a). Glob. Planet. Change 200, 103461.

Pirrone, N., Cinnirella, S., Feng, X., Finkelman, R.B., Friedli, H.R., Leaner, J., Mason, R., Mukherjee, A.B., Stracher, G.B., Streets, D.G., Telmer, K., 2010. Global mercury emissions to the atmosphere from anthropogenic and natural sources. Atmos. Chem. Phys. 10, 5951–5964.

Pisarzowska, A., Rakociński, M., Marynowski, L., Szczerba, M., Thoby, M., Paszkowski, M., Perri, M.C., Spalletta, C., Schönlaub, H.-P.-P., Kowalik, N., Gereke, M., 2020. Large environmental disturbances caused by magmatic activity during the Late Devonian Hangenberg Crisis. Glob. Planet. Change 190, 103155.

Pogge Von Strandmann, P.A.E.E., Jenkyns, H.C., Woodfine, R.G., 2013. Lithium isotope evidence for enhanced weathering during Oceanic Anoxic Event 2. Nat. Geosci. 6, 668–672.

Poulain, A.J., Amyot, M., Findlay, D., Telor, S., Barkay, T., Hintelmann, H., 2004. Biological and photochemical production of dissolved gaseous mercury in a boreal lake. Limnol. Oceanogr. 49, 2265–2275.

Poulton, S.W., Henkel, S., März, C., Urquhart, H., Flögel, S., Kasten, S., Sinninghe Damsté, J.S., Wagner, T., 2015. A continental-weathering control on orbitally driven redox-nutrient cycling during Cretaceous oceanic anoxic event 2. Geology 43, 963–966.

Pyle, D.M., Mather, T.A., 2003. The importance of volcanic emissions for the global atmospheric mercury cycle. Atmos. Environ. 37, 5115–5124.

Rakociński, M., Pisarzowska, A., Corradini, C., Narkiewicz, K., Dubicka, Z., Abdiyev, N., 2021. Mercury spikes as evidence of extended arc-volcanism around the Devonian-Carboniferous boundary in the South Tian Shan (southern Uzbekistan). Sci. Rep. 11, 5708.

Rakociński, M., Książak, D., Pisarzowska, A., Marynowski, L., 2022. Mercury evidence of intense submarine volcanism and hydrothermal activity during a mid-Tournaisian anoxic event in the Carnic Alps. Gondwana Res. 109, 225–238.

Raven, M.R., Crockford, P.W., Hodgskiss, M.S.W., Lyons, T.W., Tino, C.J., Webb, S.M., 2023. Organic matter sulfurization and organic carbon burial in the Mesoproterozoic. Geochim. Cosmochim. Acta 347, 102–115.

Ravichandran, M., 2004. Interactions between mercury and dissolved organic matter - A review. Chemosphere 55, 319–331.

Reitz, A., Thomson, J., De Lange, G.J., Hensen, C., 2006. Source and development of large manganese enrichments above eastern Mediterranean sapropel S1. Paleoceanography 21, PA3007.

Rohling, E.J., Marino, G., Grant, K.M., 2015. Mediterranean climate and oceanography, and the periodic development of anoxic events (sapropels). Earth-Science Rev. 143, 62–97.

Rosati, G., Heimbürger, L.E., Melaku, C.D., Lagane, C., Laffont, L., Rijkenberg, M.J.A., Gerringa, L.J.A., Solidoro, C., Gencarelli, C.N., Hedgecock, I.M., De Baar, H.J.W., Sonke, J.E., 2018. Mercury in the black sea: new insights from measurements and numerical modeling. Global Biogeochem. Cycles 32, 529–550.

Rush, D., Talbot, H.M., Van Der Meer, M.T.J., Hopmans, E.C., Douglas, B., Damsté, J.S.S., 2019. Biomarker evidence for the occurrence of anaerobic ammonium oxidation in

the eastern Mediterranean Sea during Quaternary and Pliocene sapropel formation. Biogeosciences 16, 2467–2479.

Rydberg, J., Gälman, V., Renberg, I., Bindler, R., Lambertsson, L., Martínez-Cortizas, A., 2008. Assessing the stability of mercury and methylmercury in a varved lake sediment deposit. Environ. Sci. Technol. 42, 4391–4396.

Sanei, H., Goodarzi, F., 2006. Relationship between organic matter and mercury in recent lake sediment: The physical-geochemical aspects. Appl. Geochemistry 21, 1900–1912.

Sanei, H., Grasby, S.E., Beauchamp, B., 2012. Latest Permian mercury anomalies. Geology 40, 63–66.

Scaife, J.D., Ruhl, M., Dickson, A.J., Mather, T.A., Jenkyns, H.C., Percival, L.M.E., Hesselbo, S.P., Cartwright, J., Eldrett, J.S., Bergman, S.C., Minisini, D., 2017. Sedimentary mercury enrichments as a marker for submarine large igneous province volcanism? Evidence From the mid-cenomanian event and oceanic anoxic event 2 (late cretaceous). Geochem. Geophys. Geosyst. 18, 4253–4275.

Schlanger, S.O., Jenkyns, H.C., 1976. Cretaceous oceanic anoxic events: causes and consequences. Geol. en Mijnb. 55, 179–184.

Schuster, P.F., Krabbenhoft, D.P., Naftz, D.L., Cecil, L.D., Olson, M.L., Dewild, J.F., Susong, D.D., Green, J.R., Abbott, M.L., 2002. Atmospheric mercury deposition during the last 270 years: A glacial ice core record of natural and anthropogenic sources. Environ. Sci. Technol. 36, 2303–2310.

Schütze, M., Gatz, P., Gilfedder, B., Biester, H., 2021. Why productive lakes are larger mercury sedimentary sinks than oligotrophic brown water lakes. Limnol. Oceanogr. 66, 1316–1332.

Shen, J., Algeo, T.J., Chen, J., Planavsky, N.J., Feng, Q., Yu, J., Liu, J., 2019a. Mercury in marine Ordovician/Silurian boundary sections of South China is sulfide-hosted and non-volcanic in origin. Earth Planet. Sci. Lett. 511, 130–140.

Shen, J., Algeo, T.J., Planavsky, N.J., Yu, J., Feng, Q., Song, H.H., Song, H.H., Rowe, H., Zhou, L., Chen, J., 2019b. Mercury enrichments provide evidence of Early Triassic volcanism following the end-Permian mass extinction. Earth-Science Rev. 195, 191–212.

Shen, J., Feng, Q., Algeo, T.J., Jinling, L., Zhou, C., Wei, W., Jiangsi, L., Them, T.R., Gill, B.C., Chen, J., 2020. Sedimentary host phases of mercury (Hg) and implications for use of Hg as a volcanic proxy. Earth Planet. Sci. Lett. 543, 116333.

Shipboard Scientific Party, 2004. Site 1261. In: Erbacher, J., Mosher, D.C., Malone, M.J. (Eds.), Proceedings of the Ocean Drilling Program, 207 Initial Reports. Ocean Drilling Program, College Station. pp. 1–103.

Sinninghe Damsté, J.S., De Leeuw, J.W., 1990. Analysis, structure and geochemical significance of organically-bound sulphur in the geosphere: State of the art and future research. Org. Geochem. 16, 1077–1101.

Snow, L.J., Duncan, R.A., Bralower, T.J., 2005. Trace element abundances in the Rock Canyon Anticline, Pueblo, Colorado, marine sedimentary section and their relationship to Caribbean plateau construction and oxygen anoxic event 2. Paleoceanography 20, PA3005.

Soerensen, A.L., Sunderland, E.M., Holmes, C.D., Jacob, D.J., Yantosca, R.M., Skov, H., Christensen, J.H., Strode, S.A., Mason, R.P., 2010. An improved global model for air-sea exchange of mercury: High concentrations over the North Atlantic. Environ. Sci. Technol. 44, 8574–8580.

Sprain, C.J., Renne, P.R., Vanderkluysen, L., Pande, K., Self, S., Mittal, T., 2019. The eruptive tempo of Deccan volcanism in relation to the Cretaceous-Paleogene boundary. Science 363, 866–870.

Strode, S.A., Jaeglé, L., Selin, N.E., Jacob, D.J., Park, R.J., Yantosca, R.M., Mason, R.P., Slemr, F., 2007. Air-sea exchange in the global mercury cycle. Global Biogeochem. Cycles 21, GB1017.

Sweere, T., Hennekam, R., Vance, D., Reichart, G.J., 2021. Molybdenum isotope constraints on the temporal development of sulfidic conditions during Mediterranean sapropel intervals. Geochem. Perspect. Lett. 17, 16–20.

Takahashi, T., Sutherland, S.C., Sweeney, C., Poisson, A., Metzl, N., Tilbrook, B., Bates, N., Wanninkhof, R., Feely, R.A., Sabine, C., Olafsson, J., Nojiri, Y., 2002. Global sea–air CO_2 flux based on climatological surface ocean pCO_2, and seasonal biological and temperature effects. Deep Sea Res. Part II Top. Stud. Oceanogr. 49, 1601–1622.

Them, T.R., Jagoe, C.H., Caruthers, A.H., Gill, B.C., Grasby, S.E., Gröcke, D.R., Yin, R., Owens, J.D., 2019. Terrestrial sources as the primary delivery mechanism of mercury to the oceans across the Toarcian Oceanic Anoxic Event (Early Jurassic). Earth Planet. Sci. Lett. 507, 62–72.

Thomson, J., Higgs, N.C., Wilson, T.R.S., Croudace, I.W., De Lange, G.J., Van Santvoort, P.J.M., 1995. Redistribution and geochemical behaviour of redox-sensitive elements around S1, the most recent eastern Mediterranean sapropel. Geochim. Cosmochim. Acta 59, 3487–3501.

Tremblin, M., Khozyem, H., Adatte, T., Spangenberg, J.E., Fillon, C., Grauls, A., Hunger, T., Nowak, A., Läuchli, C., Lasseur, E., Roig, J.-Y., Serrano, O., Calassou, S., Guillocheau, F., Castelltort, S., 2022. Mercury enrichments of the Pyrenean foreland basins sediments support enhanced volcanism during the Paleocene-Eocene thermal maximum (PETM). Glob. Planet. Change 212, 103794.

Tribovillard, N., Algeo, T.J., Lyons, T.W., Riboulleau, A., 2006. Trace metals as paleoredox and paleoproductivity proxies: An update. Chem. Geol. 232, 12–32.

Tsikos, H., Jenkyns, H.C., Walsworth-Bell, B., Petrizzo, M.R., Forster, A., Kolonic, S., Erba, E., Premoli, S.I., Baas, M., Wagner, T., Sinninghe Damsté, J.S., 2004. Carbon-isotope stratigraphy recorded by the Cenomanian-Turonian Oceanic Anoxic Event: Correlation and implications based on three key localities. J. Geol. Soc. London. 161, 711–719.

Turgeon, S., Brumsack, H.J., 2006. Anoxic vs dysoxic events reflected in sediment geochemistry during the Cenomanian-Turonian Boundary Event (Cretaceous) in the Umbria-Marche Basin of central Italy. Chem. Geol. 234, 321–339.

Ullrich, S.M., Tanton, T.W., Abdrashitova, S.A., 2001. Mercury in the aquatic environment: A review of factors affecting methylation. Crit. Rev. Environ. Sci. Technol. 31, 241–293.

van Helmond, N.A.G.M., Jilbert, T., Slomp, C.P., 2018. Hypoxia in the Holocene Baltic Sea: Comparing modern versus past intervals using sedimentary trace metals. Chem. Geol. 493, 478–490.

van Helmond, N.A.G.M., Lougheed, B.C., Vollebregt, A., Peterse, F., Fontorbe, G., Conley, D.J., Slomp, C.P., 2020. Recovery from multi-millennial natural coastal hypoxia in the Stockholm Archipelago, Baltic Sea, terminated by modern human activity. Limnol. Oceanogr. 65, 3085–3097.

Van Kaam-Peters, H.M.E., Schouten, S., Köster, J., Sinninghe Damsté, J.S., 1998. Controls on the molecular and carbon isotopic composition of organic matter deposited in a Kimmeridgian euxinic shelf sea: Evidence for preservation of carbohydrates through sulfurisation. Geochim. Cosmochim. Acta 62, 3259–3283.

Van Santvoort, P.J.M., De Lange, G.J., Thomson, J., Colley, S., Meysman, F.J.R., Slomp, C.P., 2002. Oxidation and origin of organic matter in surficial Eastern Mediterranean hemipelagic sediments. Aquat. Geochem. 8, 153–175.

Vollebregt, A., van Helmond, N.A.G.M., Pit, S., Kraal, P., Slomp, C.P., 2023. Trace metals as a redox proxy in Arabian Sea sediments in and below the oxygen minimum zone. Chem. Geol. 618, 121300.

Wallace, G.T., 1982. The association of copper, mercury and lead with surface-active organic matter in coastal seawater. Mar. Chem. 11, 379–394.

Wang, Z., Tan, J., Boyle, R., Wang, W., Kang, X., Dick, J., Lyu, Q., 2020. Mercury anomalies within the lower Cambrian (stage 2–3) in South China: Links between volcanic events and paleoecology. Palaeogeogr. Palaeoclimatol. Palaeoecol. 558, 109956.

Werne, J.P., Lyons, T.W., Hollander, D.J., Formolo, M.J., Sinninghe Damsté, J.S., 2003. Reduced sulfur in euxinic sediments of the Cariaco Basin: Sulfur isotope constraints on organic sulfur formation. Chem. Geol. 195, 159–179.

Yu, R.Q., Flanders, J.R., MacK, E.E., Turner, R., Mirza, M.B., Barkay, T., 2012. Contribution of coexisting sulfate and iron reducing bacteria to methylmercury production in freshwater river sediments. Environ. Sci. Technol. 46, 2684–2691.

Zaback, D.A., Pratt, L.M., 1992. Isotopic composition and speciation of sulfur in the Miocene Monterrey Formation: Reevaluation of sulfur reactions during early diagenesis in marine sediments. Geochim. Cosmochim. Acta 56, 763–774.

Zhao, H., Grasby, S.E., Wang, X., Zhang, L., Liu, Y., Chen, Z., Hu, Z., Huang, Y., 2022. Mercury enrichments during the Carnian Pluvial Event (Late Triassic) in South China. GSA Bull. 134, 2709–2720.

Zhu, W., Song, Y., Adediran, G.A., Jiang, T., Reis, A.T., Pereira, E., Skyllberg, U., Björn, E., 2018. Mercury transformations in resuspended contaminated sediment controlled by redox conditions, chemical speciation and sources of organic matter. Geochim. Cosmochim. Acta 220, 158–179.

Zhu, G., Wang, P., Li, T., Zhao, K., Yan, H., Li, J., Zhou, L., 2021. Nitrogen geochemistry and abnormal mercury enrichment of shales from the lowermost Cambrian Niutitang Formation in South China: Implications for the marine redox conditions and hydrothermal activity. Glob. Planet. Change 199, 103449.